

Enceloscope Mission Design Final Report

Prepared by:
Advanced Space, LLC
1400 W 122nd Avenue, Suite 200
Westminster, CO 80234
Phone: 720-545-9191
Home Page: www.advancedspace.com

August 15, 2022



Table of Contents

Introduction.....	3
Executive Summary	3
Applicable Documents.....	3
Mission Design References.....	3
Ephemeris and Body Data	3
Launch Vehicle Data.....	3
High Level Functional Requirements and Mission Parameters.....	4
Mission Design	4
Interplanetary Transfer.....	4
Interplanetary Mission Design – Methods and Set-up.....	4
Transfer Summary	6
Saturn Arrival and Transfer to Titan.....	9
Interplanetary Transfer Statistical ΔV_{99} Analysis	10
Moon Tour	12
Moon Tour Mission Design – Tisserand Model Method.....	12
Moon Tour Mission Design – Ephemeris Model Method.....	15
Moon Tour Mission Design – Summary	16
Titan Tour	16
Rhea Tour.....	18
Dione Tour	20
Tethys Tour.....	21
Enceladus Tour and Insertion	23
Moon Tour Statistical ΔV_{99}	24
Stationkeeping and Science at Enceladus	25
Science Orbit.....	26
Stationkeeping.....	26
Sample Collection Rate.....	31
Transition to Post-Science Downlink Orbit.....	32
Mission Design Summary.....	34
Mission Summary and Deterministic ΔV Budget.....	34
Statistical ΔV and Mass Budgets	34
Launch Options	37
Conclusion	37
Appendix.....	40

Results from Interplanetary Transfer Global Search with pykep and pygmo	40
EVVES Transfers Departing in 2025	40
EVVES Transfers Departing in 2026	41
EVEES Transfers Departing in 2025	42
EVEEES Transfers Departing in 2025	43
EMTG Interplanetary Transfer Solutions	44
EVVES Palma ID5 Transfer	44
$V_{\infty} = 3.5$ km/s	44
$V_{\infty} = 4.0$ km/s	44
$V_{\infty} = 5.0$ km/s (unconstrained)	45
EVVES Palma ID6 Transfer	45
$V_{\infty} = 3.5$ km/s	45
$V_{\infty} = 4.0$ km/s	46
$V_{\infty} = 4.36$ km/s (unconstrained)	46
EVVES Palma ID7 Transfer	47
$V_{\infty} = 3.5$ km/s	47
$V_{\infty} = 4.0$ km/s	47
$V_{\infty} = 4.36$ km/s (unconstrained)	48
High-Fidelity Moon Tour Trajectories	48

Introduction

Executive Summary

This report describes analyses that culminate in an end-to-end mission design for a spacecraft, Enceloscope, flying to Enceladus for the ASTROBi Foundation. The goal of the mission is fly a spacecraft to and maintain a low-altitude Enceladus orbit to collect material from the moon's liquid plumes to advance humanity's understanding of the emergence of life in the Universe. The mission design consists of a multi-gravity assist interplanetary transfer to Saturn, followed by a complex moon tour which leverages many flybys of Saturnian moons to reduce the spacecraft's (Enceloscope) energy relative to Enceladus prior to insertion into the science orbit. In addition, a science orbit and stationkeeping strategy were designed which maximize the plume material collected while minimizing the stationkeeping propellant costs. Preliminary statistical ΔV analyses were performed to estimate the propellant margin required to account for insertion, navigation, and maneuver execution errors, and launch options were considered given the resulting mass budget.

This analysis was performed by Advanced Space in support of and with funding from the ASTROBi Foundation. Additional analyses were performed studying the navigation and ground system for this mission, which are summarized in independent reports.

Applicable Documents

Mission Design References

Preliminary Trajectory Design of a Mission to Enceladus – A Master's Thesis by David F. F. Palma.

N. J. Strange, S. Campagnola, and R. P. Russell. "Leveraging flybys of low mass moons to enable an Enceladus orbiter." *Advances in the Astronautical Sciences*, 135:2207–2225, 2010. ISSN 00653438.

Ephemeris and Body Data

Saturn Satellite Fact Sheet - <https://nssdc.gsfc.nasa.gov/planetary/factsheet/saturniansatfact.html>

de430 Planetary Ephemeris Model -
https://naif.jpl.nasa.gov/pub/naif/generic_kernels/spk/planets/de430.bsp

sat375 Moon Ephemeris Model -
https://naif.jpl.nasa.gov/pub/naif/generic_kernels/spk/satellites/a_old_versions/sat375.bsp

Launch Vehicle Data

https://www.arianespace.com/wp-content/uploads/2015/09/Vega-Users-Manual_Issue-04_April-2014.pdf

<https://ablspacesystems.com/wp-content/uploads/2022/06/ABL-Payload-Users-Guide-2022-V1.pdf>

<https://www.gao.gov/assets/gao-17-609.pdf>

High Level Functional Requirements and Mission Parameters

The requirements most relevant to the mission and trajectory design are listed below:

- Launch after 2025
- Begin science operations before 2040
- Utilize an MGA interplanetary transfer which minimizes spacecraft ΔV
- Utilize a Saturnian moon tour to minimize spacecraft ΔV
- Execute autonomous stationkeeping in the science collection phase, conducting small and simple maneuvers frequently between 2 and 100 km above the surface of Enceladus

Mission Design

Interplanetary Transfer

Interplanetary Mission Design – Methods and Set-up

The goal of the interplanetary mission design was to find a minimal ΔV transfer from Earth to Saturn that launches after 2025 and arrives at Saturn with sufficient time to complete a moon tour and begin science at Enceladus by 2040.

As a starting point, scripts were developed using the pykep Python module from ESA to recreate the interplanetary transfers found by Palma. These scripts used a self-adaptive differential evolution algorithm from the pygmo Python module to solve the Multi-Gravity-Assist (MGA) optimization problem. Results from this analysis are provided in the appendix. Unfortunately, this strategy proved unsuccessful at finding the same transfers as Palma, likely due to the limited information that was available to provide the search with a good initial guess (Palma only recorded the departure and arrival epochs and C3s, no information on the timing of the gravity assists).

Next, the open-source NASA tool EMTG was leveraged to provide a more powerful and proven search for the MGA transfers. EMTG, or Evolutionary Mission Trajectory Generator, is a global trajectory optimization tool that requires minimal information as an initial guess and is designed specifically for interplanetary missions. Using this tool, the Earth-Venus-Venus-Earth-Saturn (EVVES) tours with IDs 5, 6 and 7 from Palma Table 7.2 were found. A comparison between the Palma and EMTG solutions is provided in Table 1 below:

Table 1 - Comparison between Palma and EMTG interplanetary transfers, with Earth departure V_{∞} fixed to 3.5 km/s

Solution	Palma ID5		Palma ID6		Palma ID7	
	Palma	EMTG	Palma	EMTG	Palma	EMTG
Departure Date	3/16/2026	3/21/2026	10/15/2026	10/11/2026	10/10/2026	10/9/2026
Earth Dep. C3 (km ² /s ²)	12.250	12.250	12.250	12.250	12.250	12.250
Earth Dep. V_{∞} (km/s)	3.5	3.5	3.5	3.5	3.5	3.5
Est. Earth Dep. dV (km/s)	3.767	3.767	3.767	3.767	3.767	3.767
DSM dV (km/s)	0.652	0.685	0.894	0.998	0.895	0.970
Saturn Arr. Date	10/2/2035	10/2/2035	2/23/2036	2/23/2036	9/28/2035	9/16/2035
Saturn Arrival V_{∞} (km/s)	5.943	5.947	5.943	5.944	5.964	6.000
Est. SOI dV (km/s)	0.701	0.710	0.694	0.709	0.705	0.722
Total Transfer dV (km/s)	5.120	5.162	5.113	5.474	5.367	5.459

The estimated Earth departure dV assumes the spacecraft begins in a 200x200 km altitude initial orbit and performs a single impulsive maneuver to escape Earth. The estimated Saturn Orbit Insertion (SOI) dV assumes the spacecraft arrives onto a capture orbit with a periaipse radius of 1.7 Saturn radii and an eccentricity of 0.99 with a single impulsive dV. It is expected that the differences between the Palma and EMTG solutions are primarily due to a constraint on how long after a flyby a Deep Space Maneuver (DSM) can occur and the minimum allowable flyby altitude.

The results in Table 1 above are from an EMTG search which limited the Earth departure V_{∞} to 3.5 km/s in order to match the Palma solutions as closely as possible. This search was repeated with unconstrained Earth departure conditions and improved (lower dV) solutions were found for both the ID6 and ID7 transfers. These results are shown in Table 2 below.

Table 2 - Comparison between Palma and EMTG interplanetary transfers, with an unconstrained Earth departure V_{∞}

Solution	Palma ID5		Palma ID6		Palma ID7	
	Palma	EMTG	Palma	EMTG	Palma	EMTG
Departure Date	3/16/2026	3/1/2026	10/15/2026	10/27/2026	10/10/2026	10/2/2026
Earth Dep. C3 (km ² /s ²)	12.250	25.410	12.250	19.026	12.250	19.327
Earth Dep. V_{inf} (km/s)	3.5	5.0	3.5	4.36	3.5	4.4
Est. Earth Dep. dV (km/s)	3.767	4.324	3.767	4.057	3.767	4.070
DSM dV (km/s)	0.652	0.433	0.894	0.187	0.895	0.197
Saturn Arr. Date	10/2/2035	10/16/2035	2/23/2036	2/23/2036	9/28/2035	10/30/2035
Saturn Arrival V_{inf} (km/s)	5.943	5.952	5.943	5.944	5.964	5.970
Est. SOI dV (km/s)	0.701	0.711	0.694	0.709	0.705	0.715
Est. Total Transfer dV (km/s)	5.120	5.468	5.113	4.953	5.367	4.982

The EMTG solution highlighted in green, which corresponds to the Palma transfer with ID7, was selected to be built in a higher-fidelity model and used as the baseline mission design. Although the solution with ID6 had a slightly lower total transfer ΔV , the ID7 solution arrives at Saturn nearly 4 months earlier allowing for additional time to ensure science begins at Enceladus in 2040. A graphical representation of this transfer, including a list of events, is provided in the next section in Figure 1. Graphical representations of the other EMTG solutions are provided in the Appendix.

Transfer Summary

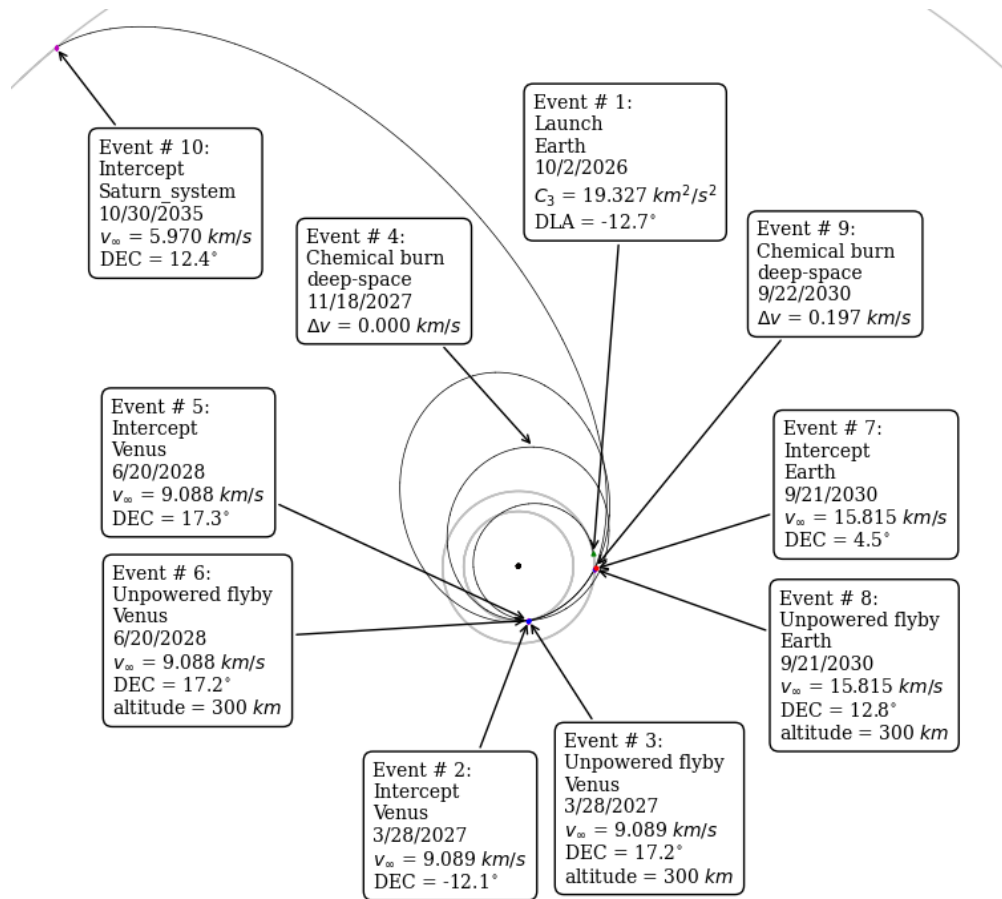


Figure 1 - EMTG solution for Palma transfer with ID7 and an unconstrained Earth departure V_{∞} , selected as the baseline interplanetary transfer

The transfer in Figure 1 was re-optimized due to two characteristics that would be operationally difficult to execute. First, the minimum flyby altitude was increased from 300 km to 500 km. 300 km was recognized as too low, especially for the Earth flyby since that would be below the International Space Station's altitude leading to complex collision avoidance operations. Secondly, the minimum time between a flyby and DSM was increased from 1 to 7 days to allow for post-flyby navigation prior to planning and executing maneuvers. The updated transfer is shown in Figure 2, with an increase in DSM dV from 197 to 300 m/s.

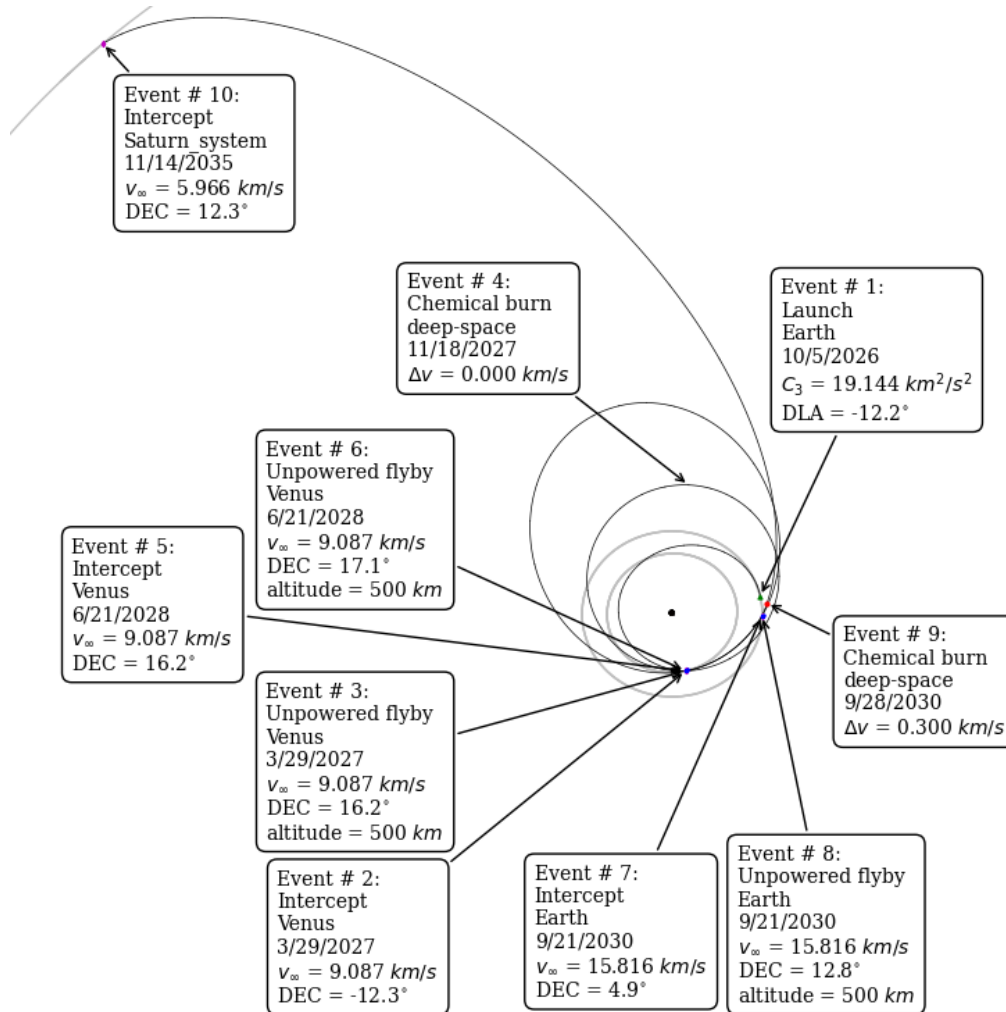


Figure 2 - EMTG solution for Palma transfer with ID7, an unconstrained Earth departure V_{∞} , increased minimum flyby altitude (500 km from 300 km), and increased minimum time between flybys and DSMs, selected as the baseline interplanetary transfer

Using the EMTG solution as an initial guess, the interplanetary transfer was recreated in Copernicus, a high-fidelity trajectory design and optimization tool developed by NASA Johnson. The force model includes point masses for the Sun, Earth, Venus, Saturn, and Jupiter's Barycenter. The Sun and planetary parameters and trajectories were read from the de430 ephemeris from JPL. The propagator used was the Livermore Solver for Ordinary Differential Equations (LSODE) with a relative and absolute error tolerance of 10E-12. The converged trajectory, which was optimized using the Sparse Nonlinear OPTimizer (SNOPT) to minimize the total ΔV (including the interplanetary injection maneuver, deep space maneuvers and Saturn orbit insertion) is illustrated in Figure 3.

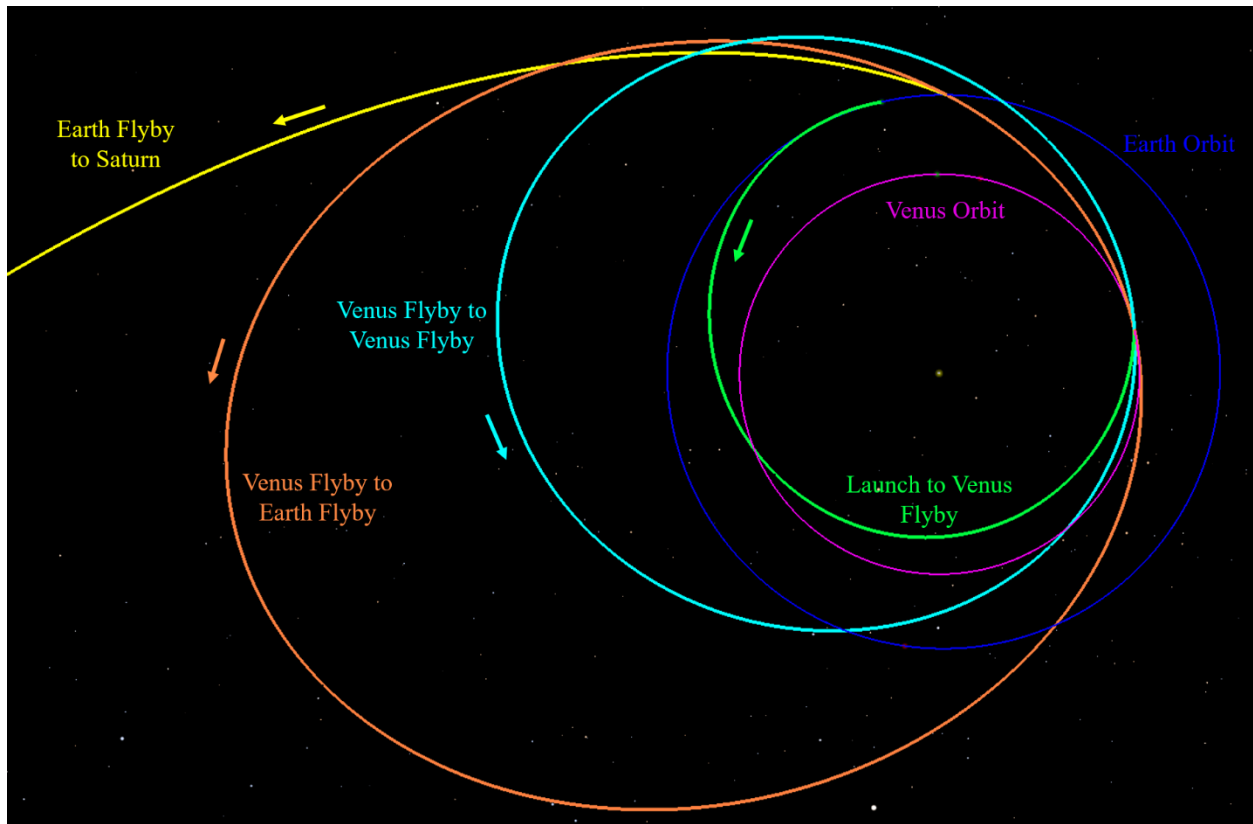


Figure 3 – Converged high-fidelity EVVES transfer in Copernicus.

The high-fidelity trajectory begins in a 200x200 km altitude low Earth orbit (LEO) at an inclination of 28.5°. The Right Ascension of the Ascending Node (RAAN) and Argument of Periapsis (AoP) of the starting orbit were part of the optimization. The initial orbit parameters are included in Table 3.

Table 3 – High-fidelity interplanetary trajectory initial orbit parameters in an Earth-centered J2000 frame.

<i>Perigee Altitude [km]</i>	<i>Apogee Altitude [km]</i>	<i>RAAN [deg]</i>	<i>AoP [deg]</i>	<i>Inclination [deg]</i>
200	200	94.440	66.875	28.5

The flybys and maneuvers in this optimized, high-fidelity trajectory are outlined in Table 4 and Table 5. Notice the flybys are all at altitudes of 500 km, which was the constrained minimum, meaning the spacecraft is leveraging as much energy as allowed from each flyby. The maneuvers labeled Deep Space Maneuvers (DSMs) in Table 5 are deterministic maneuvers in the reference trajectory. In the $\Delta V99$ study described in a later section, the small magnitude DSMs listed here, like DSM 1 and DSM 2, are renamed to Trajectory Correction Maneuvers (TCMs) since they have similar magnitudes to statistical TCMs.

Table 4 – High-fidelity interplanetary flybys, states provided in planet-centered J2000 inertial frame.

<i>Flyby</i>	<i>Epoch (UTC)</i>	V_{∞} [km/s]	<i>RA [deg]</i>	<i>DEC [deg]</i>	<i>RAAN [deg]</i>	<i>Altitude [km]</i>
<i>Venus 1</i>	29-Mar-2027 14:05:00	9.081	-74.899	-12.216	-60.471	500.0
<i>Venus 2</i>	20-Jun-2028 22:22:42	9.083	-40.836	16.248	-104.095	500.0
<i>Earth</i>	21-Sep-2030 12:49:19	15.817	3.530	4.785	-7.594	500.0

Table 5 – High-fidelity interplanetary maneuvers. ΔV components in the J2000 inertial frame.

<i>Maneuver</i>	<i>Epoch (UTC)</i>	ΔV [m/s]	ΔV_X [m/s]	ΔV_Y [m/s]	ΔV_Z [m/s]
<i>Injection</i>	05-Oct-2026 05:55:41	4064.492	-1109.283	-3835.285	761.689
<i>DSM 1</i>	31-Jan-2027 12:18:13	5.991	0.155	4.833	3.538
<i>DSM 2</i>	14-Nov-2027 13:48:04	1.539	0.624	0.257	1.383
<i>DSM 3</i>	21-Sep-2030 12:49:19	310.456	13.085	275.149	143.195
<i>DSM 4</i>	13-Feb-2033 16:51:06	38.513	-0.614	-34.497	-17.113
Total ΔV		4420.991			

Saturn Arrival and Transfer to Titan

Saturn Orbit Insertion (SOI) occurs on November 12, 2035. The insertion maneuver occurs at a periapse altitude of 160,000 km, midway between the “Janus” and “G” rings of the Saturn system. Although this high-altitude insertion isn’t the most efficient, it is necessary to minimize the risk of colliding with particles in the rings. After the 928.64 m/s SOI, the spacecraft is in a Saturn-centered orbit with an apoapse radius of approximately 16.3 million km, an orbital period of 279.3 days, and an inclination that is approximately 36.5° above Titan’s orbital plane. In order to set-up the first Titan flyby, a periapse-raising and inclination-lowering maneuver is required. This Periapse Raising Maneuver (PRM) is set to occur on January 26, 2036, with a total ΔV of 524.06 m/s. The timing, magnitude and direction of the SOI and PRM were optimized along with the Titan tour described in the Moon Tour section below.

Table 6 – Saturn Orbit Insertion (SOI) and Periapse Raising Maneuver in the high-fidelity trajectory. ΔV components in the J2000 inertial frame.

<i>Maneuver</i>	<i>Epoch (UTC)</i>	ΔV [m/s]	ΔV_X [m/s]	ΔV_Y [m/s]	ΔV_Z [m/s]
<i>Saturn Orbit Insertion (SOI)</i>	12-Nov-2035 18:26:02	928.640	-271.156	837.312	296.235
<i>Periapse Raising Maneuver (PRM)</i>	26-Jan-2036 23:01:19	524.062	-83.384	-485.869	177.819
Total ΔV		1452.703			

All the maneuvers in the interplanetary trajectory are modeled as impulsive so the trajectory is not dependent on changes to the spacecraft’s mass or thrust. Modeling the DSMs and PRM as impulsive is a reasonable assumption since the maneuvers occur in deep space, far from any gravitational body. Although the injection maneuver is a large maneuver that occurs at a low altitude near Earth, this burn can be split into multiple maneuvers to minimize the finite burn losses. The Saturn Orbit Insertion maneuver is an exception because it is a large maneuver that

cannot be split. Using an analytical method developed by Robbins¹, an upper bound for the finite burn losses on SOI was estimated for thrust levels between 10 and 100 N. The spacecraft mass prior to SOI was assumed to be 233 kg, based on a 4-stage spacecraft design that is discussed later in this report.

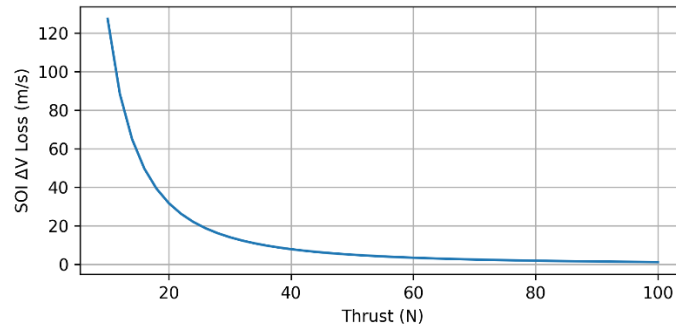


Figure 4 - Saturn Orbit Insertion finite burn losses assuming an initial mass of 233 kg.

An interplanetary spacecraft with an initial wet mass on the order of several thousand kilograms and chemical thrust should be expected to have a thrust level of at least 50 N. Since the estimated finite burn loss for thrust levels above 50 N is less than 5 m/s, which is an insignificant portion of the total ΔV , no additional ΔV was allocated to account for the impulsive burn assumption for SOI.

Interplanetary Transfer Statistical ΔV_{99} Analysis

The maneuvers and their ΔV s described thus far are deterministic, meaning they are non-zero maneuvers that exist in the reference trajectory. In addition to these deterministic maneuvers, it is important to estimate the amount of statistical ΔV that the spacecraft will require to actually fly the reference trajectory in the presence of errors. This type of analysis ensures sufficient margin is included in the propellant budget. The industry standard is to include enough propellant such that the spacecraft will have sufficient margin to complete the required ΔV with a probability of 99%. The errors in the analysis include launch or injection errors (either from the launch vehicle or the spacecraft's own injection burn), navigation errors (the uncertainty associated with not knowing *exactly* where the spacecraft is when planning correction maneuvers), and maneuver execution errors (errors in how accurately the spacecraft executes the planned deterministic and statistical maneuvers).

To estimate the ΔV required to account for these errors, a statistical ΔV_{99} analysis is performed. This analysis simulates flying the mission hundreds or thousands of times with the errors described above accounted for. Trajectory Correction Maneuvers, or TCMs, are planned along the trajectory to keep the spacecraft near the reference. In each simulation, there is a navigation and truth spacecraft. The truth spacecraft represents the actual state of the spacecraft in space, while the navigation spacecraft represents the ground (or the spacecraft's own) best estimate of the spacecraft's state. TCMs are planned using the navigation spacecraft and executed, with errors, by the truth spacecraft. Each simulation runs "end-to-end" for the interplanetary phase, beginning after the interplanetary injection maneuver and ending just before Saturn Orbit Insertion. The ΔV

¹ An Analytical Study of the Impulsive Approximation, Howard M. Robbins. AIAA Journal Vol. 4, No. 8. <https://arc.aiaa.org/doi/10.2514/3.3687>

for each TCM (and DSMs, which are re-designed in each simulation to also correct for errors) is recorded, as well as the sum of the total ΔV used in the transfer.

This ΔV_{99} analysis was completed in JPL’s MONTE software, a high-fidelity trajectory design and simulation tool. Because this analysis was performed in a different tool than the reference trajectory was designed in (Copernicus), it also serves as a verification of the reference trajectory. In the simulation, random errors are sampled from a Gaussian distribution for launch/injection, maneuver execution, and navigation state errors. Launch or injection errors (1-sigma) were defined to be $0.15 \text{ km}^2/\text{sec}^2$ for characteristic energy and 0.15° for right ascension and declination of the outgoing V_∞ vector. Maneuver execution errors (1-sigma) were defined to be 1% error in ΔV magnitude and 1° of error in ΔV direction. These errors were informed by previous missions that the Advanced Space team has worked on involving an interplanetary departure and chemical propulsion system. Navigation errors (1-sigma) were conservatively defined as 33.33 km in position and 3.33 cm/s in velocity. These navigation errors represent the steady-state uncertainty using optical only navigation from this report’s corresponding navigation study. Each TCM and DSM is optimized independently as an impulsive maneuver using the Sparse Nonlinear OPTimizer (SNOPT), with problem objective set to minimize ΔV . Constraints are included so that the maneuvers are aimed at the next flyby’s B-Plane parameters (B-dot-T and B-dot-R) and time of periapse from the reference trajectory designed in Copernicus. The mean (ΔV_μ) and 99th percentile (ΔV_{99}) for each maneuver, as well as for the total mission are shown in Table 7.

Table 7 – Mean (ΔV_μ) and 99th percentile (ΔV_{99}) values for the magnitudes of the interplanetary DSMs and TCMs from the statistical ΔV_{99} Monte Carlo analysis with 1500 trials.

<i>Journey Leg</i>	<i>Time Relative to Flybys</i>	<i>Maneuver</i>	<i>Epoch (UTC)</i>	<i>ΔV_μ [m/s]</i>	<i>ΔV_{99} [m/s]</i>
Earth to Venus 1	Launch + 21 days	TCM-1	26-Oct-2026	18.991	43.393
	Venus 1 - 88 days	TCM-2	31-Dec-2026	0.92	3.123
	Venus 1 - 57 days	TCM-3	31-Jan-2027	0.055	0.134
	Venus 1 - 21 days	TCM-4	08-Mar-2027	0.049	0.109
	Venus 1 - 7 days	TCM-5	22-Mar-2027	0.067	0.173
Venus 1 to Venus 2	Venus 1 + 21 days	TCM-6	19-Apr-2027	6.05	13.211
	Venus 2 - 224 days	TCM-7	09-Nov-2027	0.281	0.979
	Venus 2 - 219 days	TCM-8	14-Nov-2027	0.043	0.094
	Venus 2 - 21 days	TCM-9	30-May-2028	0.053	0.12
	Venus 2 - 7 days	TCM-10	13-Jun-2028	0.069	0.178
Venus 2 to Earth	Venus 2 + 21 days	DSM-1	11-Jul-2028	22.388	42.251
	Earth 2 - 411 days	TCM-11	06-Aug-2029	0.735	2.237
	Earth 2 - 21 days	TCM-12	31-Aug-2030	0.375	1.408
	Earth 2 - 7 days	TCM-13	14-Sep-2030	0.075	0.193
Earth 2 to Saturn	Earth 2 + 3 days	DSM-2	24-Sep-2030	327.488	379.1
	Earth 2 + 21 days	TCM-14	12-Oct-2030	5.545	46.284
	Saturn - 942 days	TCM-15	13-Feb-2033	0.379	5.634
	Saturn - 909 days	TCM-16	18-Mar-2033	0.057	0.28
	Saturn - 21 days	TCM-17	23-Aug-2035	0.062	0.239
	Saturn - 7 days	TCM-18	06-Sep-2035	4.981	34.642
Total				388.662	573.783

The total deterministic ΔV for the interplanetary transfer (not including the injection or SOI ΔV s) is 356.5 m/s. Under the presence of the injection, maneuver execution and navigation errors, the mean ΔV required for the transfer grew by just 32.16 m/s to 388.66 m/s. This relatively small

increase is expected and serves as a good check that the reference trajectory, designed in an independent trajectory tool, is valid. The ΔV_{99} for the interplanetary transfer was estimated to be 573.78 m/s, which represents a ΔV increase of 61% from the deterministic value. The majority of this statistical ΔV comes from the post-injection or post-flyby TCMs or DSMs, which is expected since planetary flybys tend to be the most sensitive parts of interplanetary transfers; small state errors leading into the flyby are inflated by the flyby. The current TCM placement is based on Advanced Space's experience with similar transfers but may not be completely optimal. Further investigation could result in a more optimal number and placement of TCMs. In addition, for a more accurate ΔV_{99} estimate, a "closed-loop" version of this analysis could be developed which ties the navigation simulation into this Monte Carlo, utilizing more accurate navigation covariances rather than the same Gaussian distribution at each maneuver.

In addition to the interplanetary transfer ΔV_{99} allocation, additional ΔV was added to the statistical budget to clean-up errors from the SOI and PRM, 50 and 30 m/s, respectively. These values are estimates based on Advanced Space's experience as well as data from Cassini's Saturn orbit insertion maneuver². This brings the total ΔV_{99} budget for the interplanetary transfer and insertion to 297.3 m/s, and a total ΔV budget of 6171 m/s prior to beginning the Saturnian moon tour.

Moon Tour

The Periapse Raising Maneuver (PRM) discussed above was designed to target Titan to initiate a moon tour that leverages flybys of several Saturnian moons to reduce the spacecraft's energy relative to Enceladus prior to Enceladus Orbit Insertion (EOI). If the PRM was instead designed to raise the spacecraft's Saturn-centered periapse to encounter Enceladus, insertion into a low-altitude Enceladus orbit would require an estimated 4.96 km/s of ΔV (assuming a single impulsive maneuver into a circular Enceladus orbit with a semi-major axis of 312.5 km).

In this section, it will be shown that by performing a moon tour, i.e., performing several flybys of Titan, Rhea, Dione, Tethys and finally Enceladus, the required ΔV to get the spacecraft from the post-PRM orbit to an Enceladus science orbit can be reduced to 1540 m/s, or even further with additional optimization.

Moon Tour Mission Design – Tisserand Model Method

The moon tour presented here was designed using techniques developed by Nathan Strange, Stefano Campagnola, and Ryan Russel in their paper, "Leveraging Flybys of Low Mass Moons to Enable an Enceladus Orbiter". In summary, resonant and non-resonant flybys are selected which traverse a Tisserand plot from one moon to the next. A Tisserand plot for Saturnian moons is shown in Figure 5.

² Cassini Navigation Performance Assessment. Duane Roth, Sonia Hernandez, Sean Wagner. Jet Propulsion Laboratory, March 2021. DESCANSO Deep Space Communications Navigation Systems Center of Excellence. https://descanso.jpl.nasa.gov/DPSummary/DESCANSO17_Cassini_RevA.pdf

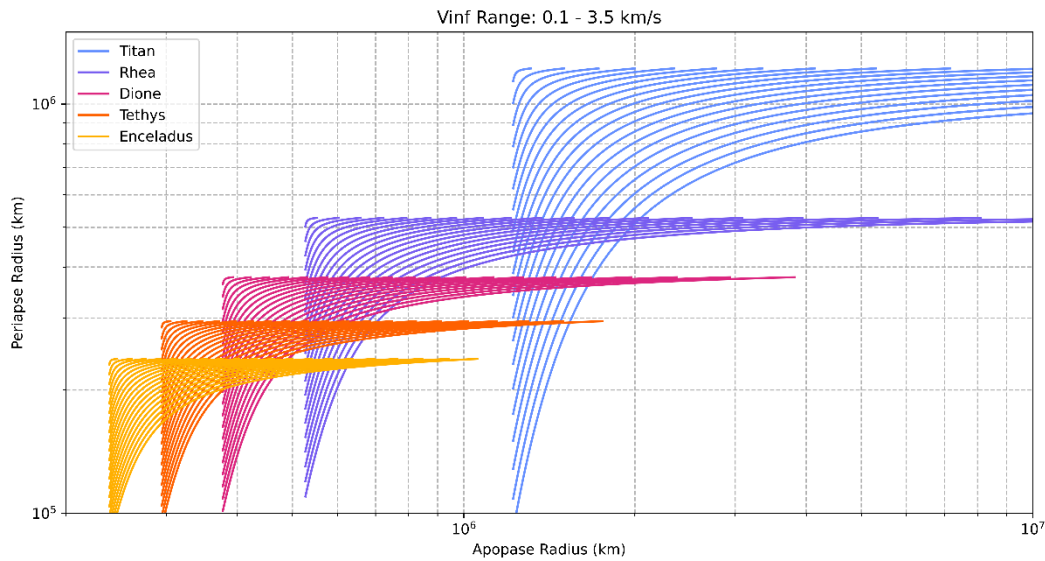


Figure 5 – Tisserand plot for the Saturn moon tour

Each curve on the Tisserand plot represents a set of orbits with varying Saturn-centered periapse and apoapse radii with a constant V_∞ with respect to the moon. Flybys of the moon may be utilized to reduce both apoapse and periapse, moving along a line of constant V_∞ . Lower altitude flybys move further along the V_∞ curve, and flybys with specific altitudes may be chosen such that the post-flyby orbital period sets up another flyby. This is done by matching a resonance with the moon’s period, such that after the flyby, the spacecraft traverses some integer value of complete revolutions while the moon completes another integer value of complete revolutions and the spacecraft re-encounters the moon at the same spot in the moon’s orbit. Another option is a non-resonant flyby, in which the spacecraft and moon re-encounter at the other crossing of the moon’s orbit. Resonant transfers are classified to have “OO” or “II” geometry. For “II” transfers the spacecraft encounters the moon when it is traversing “Inbound”, from the outside to the inside of the moon’s orbit, while for “OO” transfers the spacecraft encounters the moon while traversing “Outbound”, from the inside to outside of the moon’s orbit. This is illustrated in Figure 6. Both “Inbound” and “Outbound” flybys are designed to reduce the spacecraft’s energy.

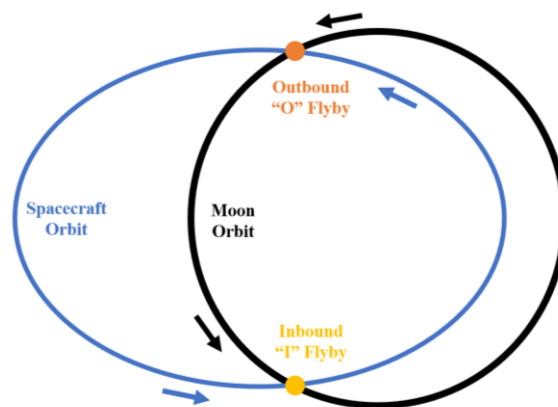


Figure 6 – Illustration of Inbound (I) and Outbound (O) flyby geometries

In addition to these resonant and non-resonant flybys, ΔV maneuvers may be leveraged to jump from one V_∞ curve to the next by either raising or lowering apoapse or periapse. Strange et. al. call

this the V-Infinity Leveraging Technique, or VILT. By stringing together resonant, non-resonant, and VILT transfers, a series of flybys can be designed that reduces the apoapse and periapse of the spacecraft enough to reach the next moon in the Titan, Rhea, Dione, Tethys and Enceladus sequence.

To build each series of flybys, Algorithm 7 and the equations within, from Palma, were recreated. An important improvement made to this algorithm, however, was to utilize Brent's method as a root solver to quickly find the VILT maneuvers and transfers. Transfers with VILT maneuvers are found by searching through α values along a set of V_∞ curves, where α is the angle between the moon's velocity vector and the spacecraft's V_∞ vector. For each α value, the pre-VILT and post-VILT spacecraft transfer durations are calculated. If that transfer duration results in the spacecraft encountering the moon at either moon orbit crossing (an Inbound or Outbound flyby), the VILT is saved as candidate transfer. In Palma, VILTs are said to be found by searching through all α values along each V_∞ curve. The speed improvement utilized a root solver to more quickly find the α value that resulted in a candidate transfer. This sped up the algorithm by a factor of ~ 100 .

An additional important deviation from the work by Palma in this tour design is that the Branch and Bound algorithm, which Palma used to find time and ΔV nearly optimal paths along the Tisserand plot, was abandoned in favor of manually building the tours. Even with the speed improvements described above, it was found that the Branch and Bound algorithm was too computationally intensive to be useful. From each flyby, the algorithm could find hundreds to thousands of transfers to the next flyby. With some tours requiring nearly 20 flybys, the search space quickly becomes incredibly vast. Building tours manually yielded tours with similar time-of-flights and ΔV s as were found by Palma, with significantly less computation. Some automation was implemented when traversing areas of the Tisserand plot without many resonances, but in this case the search was limited to looking only two or three flybys into the future. Switching to a manual method also allowed for searching through V_∞ levels with a much smaller step size than used by Palma (0.01 km/s compared to 0.1 km/s), as well as to search through all possible resonances (up to a reasonable number of revolutions, typically 15 to 20) rather than a select few. When manually selecting the transfers to the next flyby, the following rules were used to minimize ΔV and TOF:

1. Use zero- ΔV resonant or non-resonant flybys whenever possible
2. Prioritize the lowest-altitude flybys to reduce the number of flybys overall
3. Prioritize VILTs which reduce apoapse over VILTs which raise periapse

The Tisserand model makes several assumptions which must be corrected for when building the designed tours in an ephemeris model. The orbits visiting Saturnian moons are assumed to be perfectly circular, when in reality their eccentricities vary between 0.0000 (Tethys) and 0.0292 (Titan). The Tisserand model is also unable to design transfers from one moon to the next in the sequence (transferring from Titan to Rhea, for example). These transfers can be ΔV intensive given that the inclinations of the visited moons vary between 0.00 (Enceladus) and 1.86 deg (Tethys). Finally, the Tisserand model assumes the V_∞ turn from each flyby happens instantaneously, which is not the case in a high-fidelity propagated trajectory.

Moon Tour Mission Design – Ephemeris Model Method

After each moon tour was designed in the Tisserand model, the flybys, VILT maneuvers, and transfers between flybys were converted to Copernicus.

In Copernicus, a multi-shooting optimization method was used to create a nearly continuous trajectory for each moon tour. Each flyby acted as a control point, with an initial guess for the flyby state from the Tisserand solutions V_∞ and α (where α is the angle between the spacecraft's V_∞ -in vector and the moon's velocity vector at the flyby). From each flyby, a trajectory was propagated forward and backwards for half the duration to the next and previous flyby. Constraints were added such that the forward and back propagated segments from each flyby would meet and be continuous in position, velocity, and time. These constraints were set to be met near apoapse, where the forward and back propagated trajectories are least sensitive to changes at the flybys, or control points. The optimizer used was the Sparse Nonlinear OPTimizer (SNOPT) with a Finite Differences gradient method.

To ensure the moon tour in Copernicus converged to the same solution as the tour in the Tisserand model, the first Copernicus optimization fixed the timing of each flyby, as well as the VILT maneuvers' epochs, magnitudes, and directions. This over-constrained the optimization problem but doing so led to a better initial guess for the full optimization problem.

Once a good initial guess was built (evaluated by visually inspecting the forward and back propagated segments and ensuring their endpoints were in the same region of the Saturn system), the timing of the flybys and VILT maneuvers were turned on as optimization variables. From here, the Copernicus model was passed to a powerful Amazon Web Services instance to be solved. Several copies of the model were created, one for each thread of a 48-thread machine. Each copy's optimization problem and solver were then configured with semi-random values for the major optimization step limit, the optimization variable randomization percentage, and scale factors for each optimization variable. Scale factors were chosen to randomly be either 1x, 2x or 1+1x the value of the optimization variable. SNOPT major step limits were chosen to be between 0.0001 and 0.005, and the optimization variable randomization before each solve attempt was chosen to be between 0.1 and 4%. The optimization variable randomization serves to slightly "bump" each optimization variable prior to the solve attempt to prevent the problem from getting stuck in local minimums. After each set of solve attempts, the "best" solution was chosen to seed the next 48 copies, and this process was repeated until the solution was no longer improving significantly. The "best" solution was defined as the solution which had the minimum total velocity discontinuity summed between all the forward and back propagated segments. Solutions that had a significant increase in ΔV were discarded unless those solutions were the only trajectories with decreased discontinuities.

The transition between moon tours was designed using a multi-rev Lambert solver wrapped in SNOPT. From the last flyby, the trajectory was propagated forward to an MTM (Moon Transition Maneuver). This MTM was then solved with the multi-rev Lambert solver, finding a low-fidelity trajectory that intersected with the next moon. To ensure the optimal transfer was found, the time of flights between the last flyby and the MTM, and the MTM and next moon intersection, were seeded with durations of between 0 and 25 days. After each seeded optimization problem was

solved, a check was made to ensure the MTM reduced the spacecraft’s Saturn-centered semi-major axis to avoid wasting ΔV .

This MTM was used as a link between each moon tour, as each tour was set up as its own optimization problem in Copernicus. The MTM, along with a forward propagated trajectory, were manually added to the automatically built tour, and constraints were added to ensure the trajectory propagated forward from the MTM was state and time continuous with the back propagated trajectory from the first flyby.

The force model used in Copernicus for the moon tours included the Sun, Saturn, Jupiter Barycenter, Titan, Rhea, Dione, Tethys and Enceladus as point masses. The Sun, Saturn and Jupiter Barycenter parameters and trajectories were read from the de430 ephemeris, while the Saturnian moon parameters and trajectories were from the sat375 ephemeris from JPL. The propagator used was the Livermore Solver for Ordinary Differential Equations (LSODE) with a relative and absolute error tolerance of 1E-07. Figures for the high-fidelity moon tour trajectories are included in the appendix.

Moon Tour Mission Design – Summary

The completed Saturnian moon tour consists of a series of flybys of Titan, Rhea, Dione, Tethys and Enceladus over the period of 1308 days (~3.6 years). The total ΔV for the moon tour and insertion into Enceladus orbit is 1536 m/s. A summary of the tour is presented in Table 8, and details on each phase/moon are provided in the sections below.

Table 8 – Summary of the moon tour mission design – high-fidelity results. MTM: Moon Transition Maneuver. EOI: Enceladus Insertion Maneuver.

<i>Moon</i>	<i>Epoch of First Encounter</i>	<i>Number of Flybys</i>	<i>Number of VILT Maneuvers</i>	<i>TOF [days]</i>	<i>VILT ΔV [m/s]</i>	<i>MTM / EOI ΔV [m/s]</i>
<i>Titan</i>	18-Nov-2036 06:17:37	3	0	115	0.000	46.139
<i>Rhea</i>	13-Mar-2037 03:45:37	19	5	613	404.788	44.192
<i>Dione</i>	16-Nov-2038 19:49:51	11	2	184	112.669	251.776
<i>Tethys</i>	19-May-2039 12:50:12	13	4	202	154.202	210.421
<i>Enceladus</i>	07-Dec-2039 06:25:39	12	9	194	104.437	210.993
<i>Total</i>				1308	1539.617	

Titan Tour

The Titan tour begins 296 days after the PRM. Due to Titan’s relatively large mass (compared to the other Saturnian moons), only three flybys are required to lower Enceladus’s apoapse and periapse enough to encounter Rhea. Fewer flybys could have been used, as is evident by the relatively high flyby altitudes compared to the other tours, however given that the spacecraft will begin this tour after a sensitive SOI and PRM, a more conservative tour was built with more flybys at higher altitudes. This tour requires no VILTs, as Titan’s large mass allows for large turning angles that can significantly reduce the spacecraft’s period in order to reach the next resonance on the Tisserand plot. A summary of the Titan tour, as built with the Tisserand and VILT method is shown in Figure 7 and Table 9.

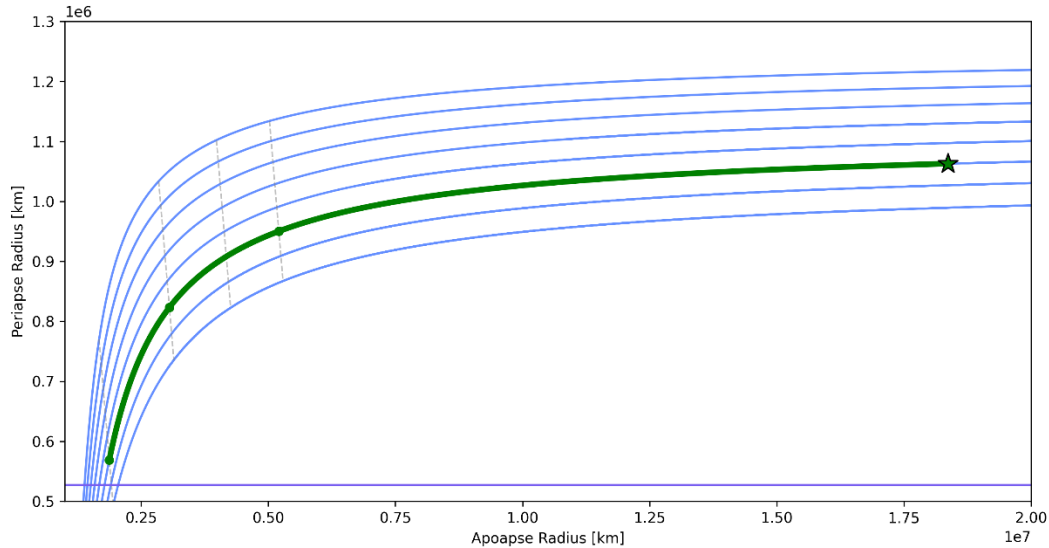


Figure 7 – Titan tour Tisserand plot. C3 curves plotted from 2.1 to 3.6 km^2/s^2 . Flybys drawn as green lines between green dots. Initial condition marked with a green star. Grey dotted lines indicate resonances.

Table 9 - Titan Tisserand tour

Flyby Number	V_∞ [km/s]	α [deg]	ΔV [m/s]	TOF [days]	Geometry	Resonance	Altitude [km]
Initial Conditions	3.10	59.50			O		
1	3.10	74.70	0.0	63.79	OO	[4, 1]	3556
2	3.10	86.88	0.0	31.89	OO	[2, 1]	5294
3	3.10	106.15	0.0	15.95	OO	[1, 1]	2073
Total			0.0	111.63			

Once the Titan tour was designed using the Tisserand method, the flybys and transfers between them were modeled in Copernicus. The Titan tour was optimized along with the SOI and PRM, with the objective of minimizing the total ΔV while creating a continuous, high-fidelity trajectory. The results of this optimization are described in Table 10.

Table 10 – High-fidelity Titan tour flybys, states provided in Titan-centered J2000 inertial frame.

Flyby Number	Epoch (UTC)	V_∞ [km/s]	RA [deg]	DEC [deg]	RAAN [deg]	Altitude [km]
1	18-Nov-2036 06:17:37	2.771	108.654	-2.332	-49.149	1821.000
2	05-Jan-2037 01:18:32	2.776	84.116	-4.484	-53.717	630.750
3	20-Jan-2037 23:26:21	2.714	52.959	-6.393	-50.517	15044.193

Once the Titan tour converged, a 3-revolution lambert arc transfer was found to set-up the first encounter of Rhea. This lambert arc was then modeled as a part of the Rhea tour and converged to a high-fidelity transfer. The resulting Moon Transition Maneuver (MTM) is described in Table 11.

Table 11 – High-fidelity Titan tour maneuvers. ΔV components in the J2000 inertial frame.

Maneuver	Epoch (UTC)	ΔV [m/s]	ΔV_X [m/s]	ΔV_Y [m/s]	ΔV_Z [m/s]
MTM to Rhea	01-Feb-2037 15:58:26	46.139	-19.249	-35.429	-22.428
Total ΔV		46.139			

The Titan tour reduces the spacecraft’s Saturn centered semi-major axis significantly, from approximately 10 million to 1.1 million km after the third flyby. If after this final flyby a periapse lowering maneuver was performed at apoapse to encounter Enceladus (at a cost of ~900 m/s), insertion into a low-altitude Enceladus science orbit would still require 3.93 km/s of ΔV (assuming a single, impulsive insertion maneuver). If Titan flybys were continued, reducing the Enceloscope’s orbit such that the apoapse radius was equal to the orbital radius of Titan and periapse radius was equal to the orbital radius of Enceladus, the Enceladus science orbit insertion would still require an estimated 3.55 km/s. These estimates motivate the design of the rest of the tour, which adds complexity and time of flight but significantly reduces the total ΔV required to achieve the science orbit.

Rhea Tour

The Rhea tour has both the longest TOF and most flybys, requiring 613 days, 19 close approaches and 445.7 m/s to reduce Enceloscope’s energy enough to encounter Dione. A summary of the Rhea tour, as built with the Tisserand and VILT method is shown in Figure 8 and Table 12.

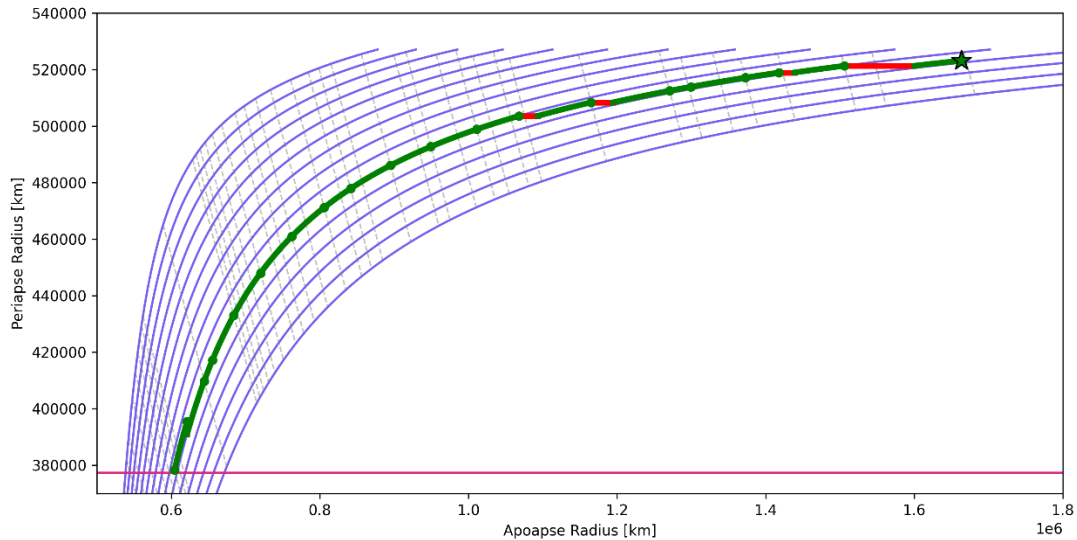


Figure 8 – Rhea tour Tisserand plot. C_3 curves plotted from 1.0 to 2.5 km^2/s^2 . Flybys drawn as green lines between green dots, with red lines denoting VILT maneuvers. Initial condition marked with a green star. Grey dotted lines indicate resonances.

Table 12 - Rhea Tisserand tour

Flyby Number	V_∞ [km/s]	α [deg]	ΔV [m/s]	TOF [days]	Geometry	Resonance	Altitude [km]
Initial Conditions	2.08	21.00			O		
1	2.00	25.82	79.8	36.15	OO	[8, 3]	131
2	1.98	30.71	19.9	22.14	OI	[4, 1]	126
3	1.98	33.84	0.0	54.22	II	[12, 5]	632
4	1.98	38.72	0.0	41.25	IO	[9, 4]	120
5	1.98	40.61	0.0	49.70	OO	[11, 5]	1581
6	1.94	45.99	38.6	18.08	OO	[4, 2]	97
7	1.90	51.45	37.8	48.86	OI	[10, 5]	126
8	1.90	55.81	0.0	54.22	II	[12, 7]	315
9	1.90	60.75	0.0	36.14	II	[8, 5]	182
10	1.90	65.36	0.0	13.55	II	[3, 2]	253

11	1.90	70.33	0.0	31.63	II	[7, 5]	178
12	1.90	73.88	0.0	18.07	II	[4, 3]	570
13	1.90	78.66	0.0	22.59	II	[5, 4]	216
14	1.90	83.91	0.0	31.63	II	[7, 6]	124
15	1.90	89.21	0.0	54.22	II	[12, 11]	117
16	1.90	94.22	0.0	25.06	IO	[5, 5]	168
17	1.90	96.43	0.0	4.52	OO	[1, 1]	1410
18	1.86	101.14	24.1	10.73	OI	[2, 2]	107
19	1.86	106.00	0.0	40.66	II	[9, 10]	243
Total			200.2	613.42			

In the converged high-fidelity Rhea tour, the total VILT maneuver ΔV increased from 200.2 to 404.8 m/s. While this is significant, this result is not totally unexpected given the significant number of flybys in this tour and necessity of the VILTs to correct for the low-fidelity assumptions of the Tisserand tour. The flybys and VILTs in the high-fidelity tour are described in Table 13 and Table 14.

Table 13 – High-fidelity Rhea tour flybys, states provided in Rhea-centered J2000 inertial frame.

Flyby Number	Epoch (UTC)	V_{∞} [km/s]	RA [deg]	DEC [deg]	RAAN [deg]	Altitude [km]
1	13-Mar-2037 03:45:37	2.037	19.764	-3.855	-136.645	63.862
2	18-Apr-2037 07:33:15	1.993	11.113	-4.341	-151.184	87.549
3	10-May-2037 10:32:09	1.989	31.234	-6.417	117.959	700.313
4	03-Jul-2037 16:19:33	1.927	32.861	-6.379	166.585	123.193
5	13-Aug-2037 21:09:24	1.940	8.982	-6.009	-43.535	1469.160
6	02-Oct-2037 14:03:23	1.967	6.036	-5.817	-51.761	503.066
7	20-Oct-2037 15:10:19	1.818	3.346	-5.665	-45.388	579.789
8	08-Dec-2037 13:36:46	2.017	39.079	-6.732	-158.178	350.402
9	31-Jan-2038 18:54:50	1.986	42.702	-8.015	-153.272	96.037
10	08-Mar-2038 22:09:00	2.017	47.713	-9.706	138.670	268.844
11	22-Mar-2038 11:22:30	2.015	51.765	-9.692	147.089	167.994
12	23-Apr-2038 02:20:18	2.013	56.478	-9.618	114.643	514.084
13	11-May-2038 04:26:18	1.977	60.550	-9.369	111.456	152.286
14	02-Jun-2038 19:21:42	1.924	67.031	-8.844	106.102	66.930
15	04-Jul-2038 10:37:55	1.906	73.277	-7.728	97.765	73.910
16	27-Aug-2038 16:04:08	1.891	79.647	-6.045	101.682	183.025
17	21-Sep-2038 17:15:47	1.863	92.413	-3.880	-58.236	1830.640
18	26-Sep-2038 05:52:26	1.901	90.955	-4.070	-58.675	464.002
19	07-Oct-2038 00:30:12	1.859	68.018	-5.802	108.276	100.000

Table 14 – High-fidelity Rhea tour maneuvers. ΔV components in the J2000 inertial frame.

Maneuver	Epoch (UTC)	ΔV [m/s]	ΔV_X [m/s]	ΔV_Y [m/s]	ΔV_Z [m/s]
VILT 1	13-Mar-2037 11:43:47	105.585	-65.687	-81.594	13.261
VILT 2	19-Apr-2037 11:24:56	42.050	-23.145	-34.740	5.060
VILT 3	02-Oct-2037 14:03:40	84.771	-82.504	-16.651	10.092
VILT 4	27-Oct-2037 17:59:48	118.816	-64.392	99.837	1.876
VILT 5	29-Sep-2038 00:51:59	53.566	-49.271	-19.807	7.023
MTM to Dione	19-Oct-2038 10:33:44	44.192	0.548	-5.295	43.871
Total ΔV		448.980			

Dione Tour

The Dione tour and transfer to Tethys requires 184 days and 364.4 m/s. A summary of the Dione tour, as built with the Tisserand and VILT method is shown in Figure 9 and Table 15

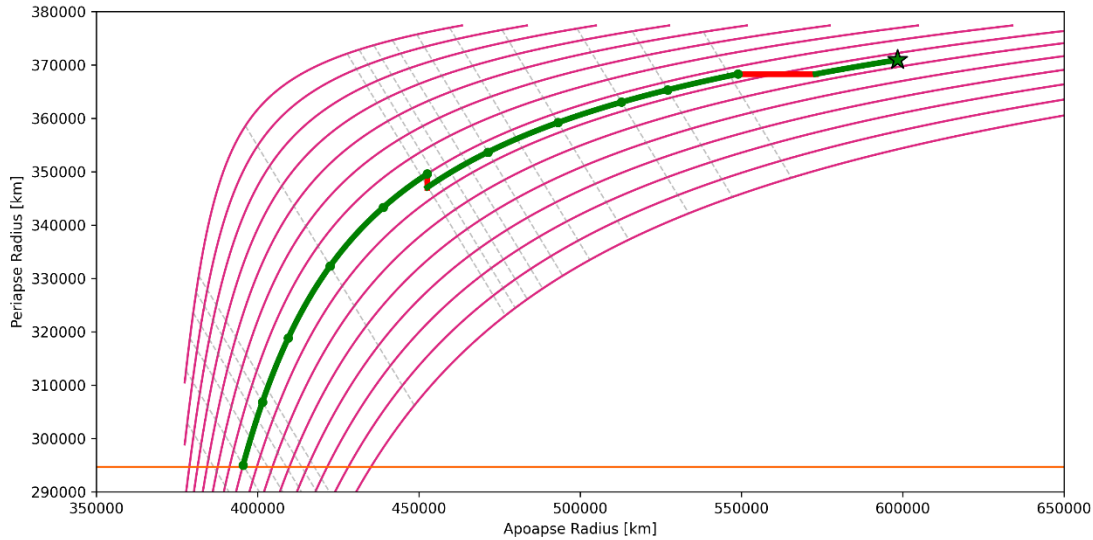


Figure 9 – Dione tour Tisserand plot. C3 curves plotted from 0.5 to 2.0 km²/s². Flybys drawn as green lines between green dots, with red lines denoting VILT maneuvers. Initial condition marked with a green star. Grey dotted lines indicate resonances.

Table 15 - Dione Tisserand tour

Flyby Number	V_{∞} [km/s]	α [deg]	ΔV [m/s]	TOF [days]	Geometry	Resonance	Altitude [km]
<i>Initial Conditions</i>	1.35	41.00			I		
1	1.25	49.63	95.1	11.42	IO	[4, 3]	51
2	1.25	56.20	0.0	24.64	OO	[9, 7]	209
3	1.25	60.53	0.0	13.69	OO	[5, 4]	631
4	1.25	66.63	0.0	16.42	OO	[6, 5]	271
5	1.25	73.78	0.0	21.90	OO	[8, 7]	142
6	1.20	79.22	17.6	29.04	OI	[10, 9]	174
7	1.20	85.03	0.0	3.96	IO	[1, 1]	390
8	1.20	93.43	0.0	2.74	OO	[1, 1]	81
9	1.20	102.22	0.0	3.75	OI	[1, 1]	51
10	1.20	109.51	0.0	27.37	II	[10, 11]	186
11	1.20	116.67	0.0	19.16	II	[7, 8]	201
Total			112.7	174.09			

A notable feature of the Dione tour is that it requires a series of relatively low-altitude flybys with less than 4-days between them (flyby numbers 7 through 9). These flybys are required to traverse the area of the Tisserand plot where the only resonant and non-resonant transfers available are those with resonances close to 1:1. Due to the short timeline between these flybys, the navigation uncertainty before and after them must be reduced quickly which may require radiometric tracking with stations on Earth. The two VILT maneuvers in the high-fidelity Dione tour stayed very close to their low-fidelity estimates (staying within <0.1 m/s), while the flyby altitudes also generally stay close to the Tisserand model's tour. The flybys and VILT maneuvers in the high-fidelity tour are described in Table 16 and Table 17.

Table 16 – High-fidelity Dione tour flybys, states provided in Dione-centered J2000 inertial frame.

Flyby Number	Epoch (UTC)	V_{∞} [km/s]	RA [deg]	DEC [deg]	RAAN [deg]	Altitude [km]
1	16-Nov-2038 19:49:52	1.327	106.097	-2.977	124.734	101.259
2	28-Nov-2038 05:02:37	1.187	76.502	-5.251	-52.496	194.286
3	22-Dec-2038 20:33:41	1.196	70.737	-5.778	-36.240	604.819
4	05-Jan-2039 13:02:16	1.195	66.390	-5.756	-46.186	281.962
5	21-Jan-2039 23:34:12	1.218	60.795	-5.925	-53.525	129.781
6	12-Feb-2039 20:38:09	1.174	52.572	-6.203	-54.007	174.246
7	13-Mar-2039 22:42:37	1.218	69.754	-5.643	123.427	355.192
8	17-Mar-2039 21:36:09	1.197	65.272	-5.932	-44.131	60.572
9	20-Mar-2039 15:18:59	1.193	56.924	-6.154	-48.274	51.019
10	24-Mar-2039 09:07:58	1.207	25.344	-6.240	150.205	269.966
11	20-Apr-2039 18:00:34	1.254	31.984	-6.842	124.006	50.000

Table 17 – High-fidelity Dione tour maneuvers. ΔV components in the J2000 inertial frame.

Maneuver	Epoch (UTC)	ΔV [m/s]	ΔV_X [m/s]	ΔV_Y [m/s]	ΔV_Z [m/s]
VILT 1	17-Nov-2038 02:29:15	95.099	17.986	-93.233	5.286
VILT 2	13-Feb-2039 19:36:15	17.570	-3.242	17.240	-0.985
MTM to Tethys	28-Apr-2039 04:55:24	251.776	-4.442	195.111	-159.069
Total ΔV		364.445			

Tethys Tour

The Tethys tour and transfer to Enceladus requires 202 days and 364.6 m/s. A summary of the Tethys tour, as built with the Tisserand and VILT method is shown in Figure 10 and Table 18.

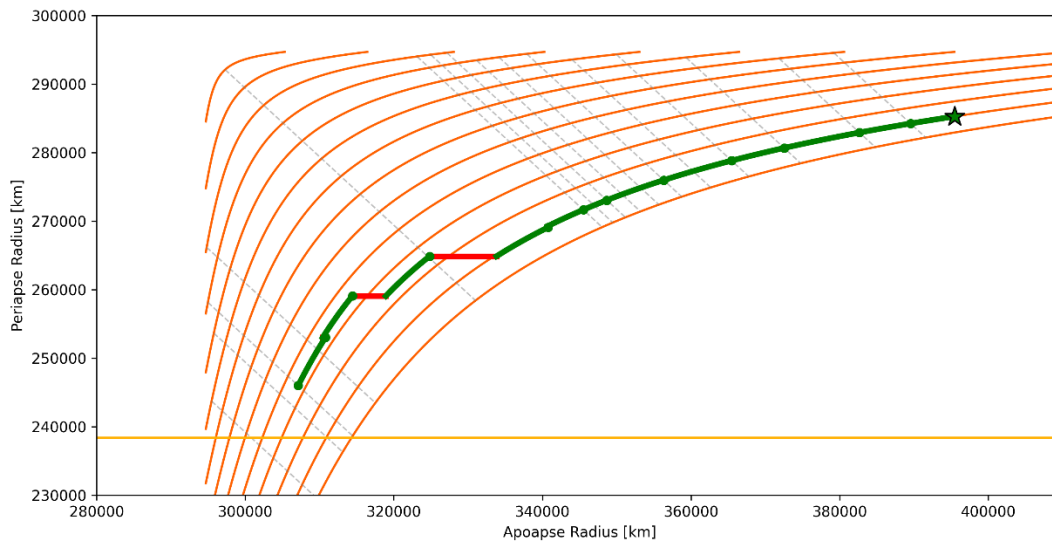


Figure 10 – Tethys tour Tisserand plot. C3 curves plotted from 0.1 to 1.5 km^2/s^2 . Flybys drawn as green lines between green dots, with red lines denoting VILT maneuvers. Initial condition marked with a green star. Grey dotted lines indicate resonances.

Table 18 - Tethys Tisserand tour

Flyby Number	V_{∞} [km/s]	α [deg]	ΔV [m/s]	TOF [days]	Geometry	Resonance	Altitude [km]
<i>Initial Conditions</i>	1.30	58.12			I		
1	1.30	60.71	0.0	20.78	II	[11, 9]	522
2	1.30	63.76	0.0	11.33	II	[6, 5]	363
3	1.30	68.35	0.0	13.22	II	[7, 6]	53
4	1.30	71.67	0.0	15.11	II	[8, 7]	285
5	1.30	76.19	0.0	18.89	II	[10, 9]	64
6	1.30	80.24	0.0	24.55	II	[13, 12]	134
7	1.30	82.02	0.0	28.33	II	[15, 14]	1020
8	1.30	84.95	2.0	2.73	IO	[1, 1]	440
9	1.15	92.79	76.8	1.92	OO	[1, 1]	63
10	1.05	101.29	40.7	2.63	OI	[1, 1]	58
11	1.06	106.79	3.4	25.83	IO	[13, 14]	160
12	1.06	113.35	0.0	18.89	OO	[10, 11]	67
Total			122.9	184.21			

Similar to the Dione tour, the Tethys tour requires a sequence of several low-altitude flybys with short transfers between them. These flybys (numbers 8 through 10), as well as relatively large VILT maneuvers, are required to traverse the area of the Tisserand plot where the resonances are near 1:1. Resonances with a high number of revolutions (greater than 20) could be used to traverse this section with less ΔV , but the time-of-flight for the tour would increase significantly putting a 2040 Enceladus arrival at risk. The flybys and VILT maneuvers in the high-fidelity tour are described in Table 19 and Table 20.

Table 19 – High-fidelity Tethys tour flybys, states provided in Tethys-centered J2000 inertial frame.

Flyby Number	Epoch	V_{∞} [km/s]	RA [deg]	DEC [deg]	RAAN [deg]	Altitude [km]
1	19-May-2039 12:50:12	1.373	85.978	-1.433	98.317	500.440
2	09-Jun-2039 07:24:02	1.336	88.540	-0.648	-101.451	375.400
3	20-Jun-2039 15:17:47	1.299	90.617	-1.204	98.617	61.384
4	03-Jul-2039 20:26:07	1.301	95.369	-1.124	-124.527	291.702
5	18-Jul-2039 23:06:09	1.281	99.596	-0.209	101.159	65.812
6	06-Aug-2039 20:24:14	1.265	105.515	0.844	99.978	127.619
7	31-Aug-2039 09:17:50	1.304	109.465	1.116	93.993	1041.973
8	28-Sep-2039 16:53:48	1.282	111.047	0.329	-64.051	481.606
9	01-Oct-2039 10:17:30	1.204	103.886	-2.720	-7.296	88.847
10	03-Oct-2039 07:34:10	1.172	94.827	-2.774	-65.189	273.599
11	05-Oct-2039 22:59:08	1.031	73.383	-4.911	102.937	195.126
12	31-Oct-2039 18:55:26	0.980	108.991	-0.495	-43.882	78.947
13	19-Nov-2039 15:58:00	0.985	101.444	0.174	-79.940	80.446

Table 20 – High-fidelity Tethys tour maneuvers. ΔV components in the J2000 inertial frame.

Maneuver	Epoch (UTC)	ΔV [m/s]	ΔV_X [m/s]	ΔV_Y [m/s]	ΔV_Z [m/s]
VILT 1	28-Sep-2039 07:11:10	7.219	-0.226	-7.188	0.627
VILT 2	01-Oct-2039 09:17:52	47.834	46.935	-8.592	-3.373
VILT 3	02-Oct-2039 22:26:56	93.991	23.640	-90.812	5.361
VILT 4	05-Oct-2039 20:04:38	5.158	3.742	2.941	-1.989
MTM to Enceladus	21-Nov-2039 22:10:10	210.421	-38.007	18.440	206.137
Total ΔV		364.623			

Enceladus Tour and Insertion

The Enceladus tour is unique in that it is no longer the goal to reduce the periapse and apoapse radius to reach the next moon, but instead to purely reduce Enceladus's V_∞ with respect to Enceladus. In order to most efficiently reduce the V_∞ , periapse *raising* maneuvers, unintuitively, are used in combination with several low-altitude flybys. In the designed tour, 112.2 m/s and 13 flybys are leveraged to reduce V_∞ from 0.74 to 0.33 km/s. A summary of the Enceladus tour, as built with the Tisserand and VILT method is shown in Figure 11 and Table 21.

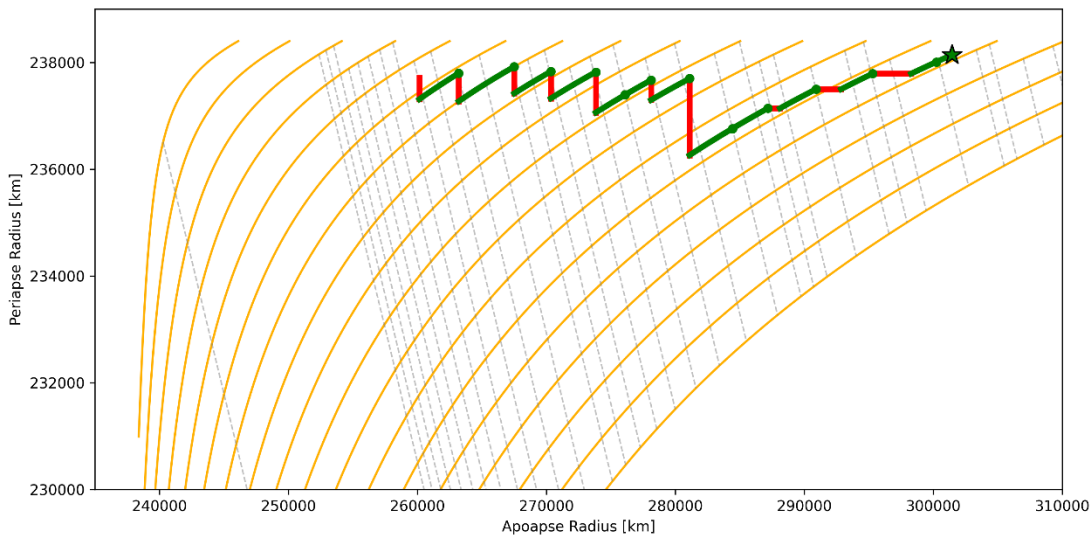


Figure 11 – Enceladus tour Tisserand plot. C3 curves plotted from 0.1 to 1.0 km^2/s^2 . Flybys drawn as green lines between green dots, with red lines denoting VILT maneuvers. Initial condition marked with a green star. Grey dotted lines indicate resonances.

Table 21 - Enceladus Tisserand tour

Flyby Number	V_∞ [km/s]	α [deg]	ΔV [m/s]	TOF [days]	Geometry	Resonance	Altitude [km]
<i>Initial Conditions</i>	0.74	15.70			O		
1	0.74	19.33	0.0	8.17	OI	[5, 4]	150
2	0.71	24.53	29.9	17.97	IO	[13, 11]	54
3	0.69	30.07	19.9	9.62	OO	[7, 6]	53
4	0.68	35.56	9.9	20.61	OO	[15, 13]	64
5	0.68	40.26	0.0	10.99	OO	[8, 7]	112
6	0.57	29.15	18.3	23.20	OI	[16, 14]	71
7	0.54	30.50	4.7	12.38	II	[9, 8]	85
8	0.54	35.57	0.0	26.11	II	[19, 17]	283
9	0.48	28.82	9.7	13.77	II	[10, 9]	276
10	0.44	29.81	6.5	15.14	II	[11, 10]	79
11	0.40	28.65	6.5	16.63	IO	[12, 11]	196
12	0.36	33.66	6.8	19.07	OI	[13, 12]	62
Total			112.2	193.66			

The high-fidelity Enceladus tour was optimized along with the Enceladus Orbit Insertion (EOI) maneuver, with the objective of minimizing the sum of the ΔV s for the VILT maneuvers and EOI. This tour matched the Tisserand tour most closely out of all the tours. The total ΔV for the VILT maneuvers decreased from 112.2 to 104.5 m/s, and the flyby altitudes stayed within 10-20 km of

the lower-fidelity model’s solution. The flybys, VILT maneuvers, and EOI are outlined in Table 22 and Table 23.

Table 22 – High-fidelity Enceladus tour flybys, states provided in Enceladus-centered J2000 inertial frame.

<i>Flyby Number</i>	<i>Epoch (UTC)</i>	<i>V_∞ [km/s]</i>	<i>RA [deg]</i>	<i>DEC [deg]</i>	<i>RAAN [deg]</i>	<i>Altitude [km]</i>
1	07-Dec-2039 06:25:39	0.731	74.931	-4.789	-69.553	144.361
2	15-Dec-2039 10:00:24	0.732	91.107	-4.164	139.740	59.545
3	02-Jan-2040 08:09:13	0.710	73.015	-5.404	-50.673	62.920
4	11-Jan-2040 22:18:21	0.688	67.386	-5.678	-53.034	64.914
5	01-Feb-2040 11:32:58	0.666	62.853	-5.978	-44.898	113.043
6	12-Feb-2040 10:57:33	0.702	56.912	-6.267	-42.519	77.910
7	06-Mar-2040 13:27:27	0.566	83.706	-4.791	125.266	73.307
8	18-Mar-2040 21:40:30	0.553	91.489	-4.097	119.582	287.731
9	13-Apr-2040 23:07:27	0.500	95.161	-3.501	128.802	271.244
10	27-Apr-2040 16:34:09	0.447	95.463	-3.526	134.376	88.929
11	12-May-2040 18:26:59	0.422	98.704	-3.556	128.644	210.424
12	29-May-2040 08:31:51	0.397	77.110	-5.157	-19.732	65.482

Table 23 – High-fidelity Titan tour maneuvers. ΔV components in the J2000 inertial frame.

<i>Maneuver</i>	<i>Epoch (UTC)</i>	<i>ΔV [m/s]</i>	<i>ΔVX [m/s]</i>	<i>ΔVY [m/s]</i>	<i>ΔVZ [m/s]</i>
VILT 1	15-Dec-2039 08:40:04	17.700	-10.062	-14.457	1.748
VILT 2	02-Jan-2040 08:32:43	23.132	3.210	-22.835	1.836
VILT 3	16-Jan-2040 13:35:21	15.594	-6.896	-13.901	1.542
VILT 4	21-Feb-2040 22:10:04	11.843	8.832	-7.877	0.448
VILT 5	06-Mar-2040 11:36:18	4.667	3.943	2.353	-0.835
VILT 6	15-Apr-2040 08:44:54	10.015	8.517	5.166	-1.043
VILT 7	28-Apr-2040 21:19:21	7.774	-7.652	1.126	0.780
VILT 8	14-May-2040 13:47:45	0.770	-0.470	0.350	0.499
VILT 9	03-Jun-2040 00:03:39	12.978	12.080	-4.643	-0.958
EOI	17-Jun-2040 10:19:06	210.993	68.601	196.097	36.851
Total ΔV		315.465			

The EOI maneuver, which occurs on June 17, 2040, is a 211 m/s maneuver which occurs entirely in the anti-velocity direction relative to Enceladus and places the spacecraft in a circular orbit with a semi-major axis of 312.5 km and inclination of 93°. For navigation purposes, this may need to be split into two or more maneuvers.

Moon Tour Statistical ΔV99

The statistical ΔV budget for the moon tour was estimated based on the results of the interplanetary statistical ΔV analysis as well as a review of the Cassini mission ΔV budget³. For the interplanetary analysis, 217 m/s of ΔV was added to the budget to account for injection, navigation, and maneuver execution errors. This represents approximately 64% of the deterministic ΔV. For the moon tour, a similar allocation would result in 850 m/s of ΔV to account for these errors.

³ Cassini Navigation Performance Assessment. Duane Roth, Sonia Hernandez, Sean Wagner. Jet Propulsion Laboratory, March 2021. DESCANSO Deep Space Communications Navigation Systems Center of Excellence. https://descanso.jpl.nasa.gov/DPSummary/DESCANSO17_Cassini_RevA.pdf

Cassini performed several low-altitude flybys of Saturnian moons, similar to the planned trajectory for Enceloscope. For the first 20 flybys, Cassini allocated an average of 12.2 m/s for a ΔV_{95} budget. A similar allocation for Enceloscope, which has 58 planned flybys, would result in 707.6 m/s of ΔV . Given that the Enceloscope spacecraft is expected to have more navigation uncertainty than Cassini, the more conservative value of 850 m/s, extrapolated from the interplanetary analysis, was chosen as the statistical ΔV budget for the moon tour.

Stationkeeping and Science at Enceladus

The science orbit has been selected through a trade of science collection and stationkeeping fuel cost. Several orbit regimes were considered including flybys, halo orbits, elliptical orbits, and near-circular orbits. The science orbit was selected to be an elliptical orbit with a specific stationkeeping corridor because it maximized the science return for each gram of fuel. The science collection occurs quickly, where it is assumed that the majority of effort is focused on collecting the science samples; the science processing and data downlink will take place in a stable orbit afterward. The main trade is summarized here.

Enceladus flybys: One can build a science campaign without entering into orbit about Enceladus by extending the moon tour about Saturn to fly through the Tiger Stripe plumes from Saturn orbit. This yields a campaign that samples plume material at some resonance with Enceladus' orbit – no more than once every Enceladus orbit but more likely less often. The lowest flyby velocities one can achieve at an altitude of 10 km are on the order of 250 m/s, but with different Enceladus orbit resonances the flyby speeds are substantially higher. It is a reasonable estimate to expect flyby speeds on the order of 350 m/s. The benefit of this sort of mission is that the flybys may be individually targeted and processing of the scientific collection may be performed immediately afterward. The primary drawbacks of this approach are the higher flyby speeds and less material collected, though there are also some challenges with ensuring safe, low-altitude flybys.

Halo orbits: Halo orbits are clearly interesting because they always pass over the Southern Pole and are designed to manage the Saturn gravitational perturbations in an elegant way. There are several types of halo orbits that one may construct, with periapses that are always located over the Southern pole. In general, the halo orbits permit one good sampling passage per Enceladus orbit, though it may be possible to build something like a near rectilinear halo orbit (NRHO) that passes through the plumes four times per Enceladus orbit. The sampling velocities are on the order of 240 m/s. Through literature (Enceladus Orbilander⁴), we see a good design for a halo orbit and stationkeeping strategy that uses about 0.6 m/s per day of ΔV during operations and flies through the plumes once every other day, yielding approximately 1.1 m/s of ΔV per science collection. The science collection altitude is 20 km in the study but can be refined. If one considers the total time below 30 km with latitudes below -70 deg, then this amounts to approximately 19 minutes per pass of science collection, amounting to approximately 17.4 minutes of science collection per 1 m/s of

⁴ Enceladus Orbilander, A Flagship Mission Concept for Astrobiology, supporting the Planetary Mission Concept Studies for the 2023-2033 Decadal Survey, Shannon MacKenzie, Karen Kirby, and Peter Greenauer, Johns Hopkins University, Applied Physics Laboratory.
https://ntrs.nasa.gov/api/citations/20205008712/downloads/enceladusorbilander_2020pmcs.pdf

ΔV . If the periapse is dropped to a very low 2 km altitude, then the spacecraft could achieve about 27 minutes of science collection per 1 m/s of ΔV .

Elliptical orbits: If one reduces the orbit to an elliptical orbit with a low periapse altitude and a higher apoapse altitude of approximately 10 km x 102 km, then the plume sampling velocities drop to 185 m/s and one can pass through the plumes multiple times per day. This will be discussed in more detail in this section. The best design to date achieves approximately 2.477 hours (148.6 min) of sampling per 1 m/s of stationkeeping fuel in the best scenarios. This is substantially higher than the halo orbit design.

Near-circular orbits: The natural extension of the elliptical orbit is to further reduce the orbit to nearly circular and low in altitude. The sampling velocity drops to approximately 173 m/s, but the stationkeeping is very challenging and expensive in fuel cost. This was deemed infeasible given the frequency and size of stationkeeping maneuvers.

Science Orbit

The science orbit selected in this study provides a high cadence of good science collection passages using a relatively low amount of fuel by carefully balancing the significant gravitational perturbations provided by Saturn's and Enceladus' gravity fields with a strategic stationkeeping strategy.

The science orbit was identified through a focused, directed survey of options. First, it was understood that the science orbit would need to have a high inclination in order to pass through the geyser plumes. Thus, orbits were only considered whose orbital inclinations were between 70 and 110 deg. The survey considered a science corridor whose periapse and apoapse altitudes were controlled, with a wide variety of corridor definitions. As the surveys progressed, the corridor definitions were refined to track the best performance. Finally, the argument of periapse was selected to work in resonance with the gravitational perturbations and yield a high number of collection passages.

Stationkeeping

The stationkeeping strategy implemented in this reference uses a variety of triggers to raise or lower the spacecraft's velocity. No plane changing is presently implemented in order to save fuel; the plane certainly changes rapidly under the influence of gravity. Hence, careful monitoring of the orbital period and altitude controls the orbital plane using less fuel.

The logic employed works thus:

- If the periapse altitude drops below 2 km, then raise it to 7.76 km with a stationkeeping maneuver executed the previous apoapse.
- If the periapse altitude exceeds 106 km, then lower it to 7.76 km. This logic is not triggered but is used to explain that the periapse may grow high and that is acceptable.
- If the apoapse altitude exceeds 96.5 km, then lower it to 96.5 km with a stationkeeping maneuver executed the previous periapse.
- The apoapse altitude is permitted to be as low as it evolves without a trigger to raise it.

Other variations were considered as well, including lowering the periapse intentionally when the periapse is over the South Pole, but that increased the fuel use without increasing the science

collection rate sufficiently. It is expected that small adjustments in the mean semimajor axis may assist at maintaining the resonance closer, and this has been identified as an area for future work.

The altitude of the orbit over time is illustrated in Figure 12, with stationkeeping maneuvers and science collection passages indicated. The gray curves are time profiles if no stationkeeping maneuvers are executed, and stationkeeping maneuvers are introduced when the altitude profile triggers one.

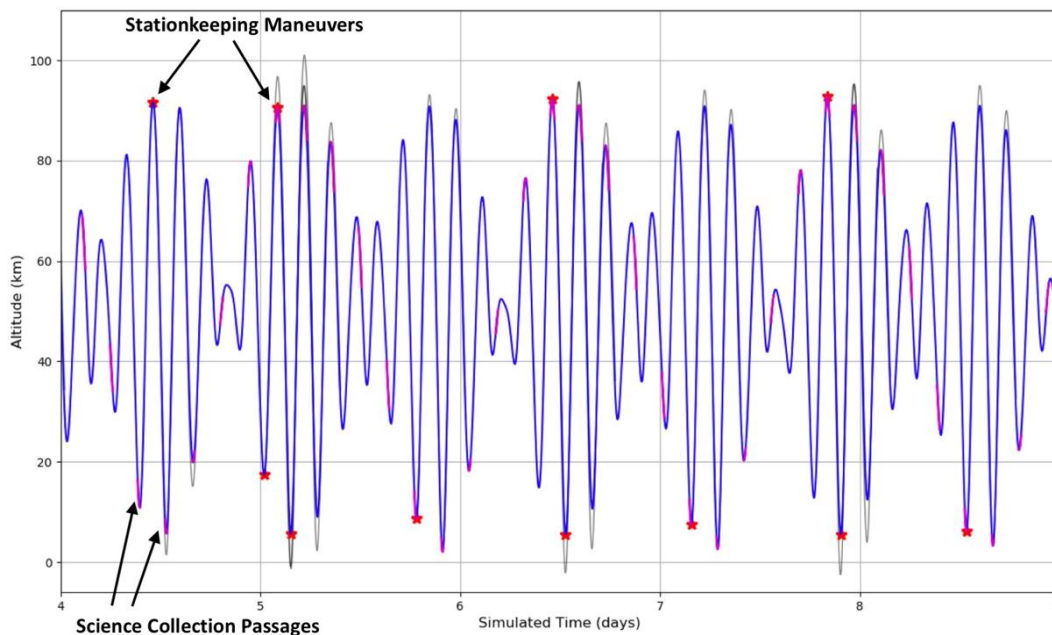


Figure 12 – The altitude of the orbit over time, with stationkeeping maneuvers and science collection passages indicated.

The science orbit evolves rapidly under the influence of the Saturn and Enceladus gravity fields. Figure 13 illustrates the semi-major axis, argument of periapse, inclination, and longitude of the ascending node of the orbit over time in Enceladus-centered inertial coordinates. One sees that the semi-major axis has an average of approximately 312.5 km, which places this orbit very nearly into a 10:1 resonance, such that the orbiter revolves about Enceladus approximately 10 times for each revolution of Enceladus about Saturn.

The inclination of the orbit varies by about 5 degrees each revolution, when computed instantaneously at each propagation step, though the secular trend is very small. It may be possible to improve the orbit performance slightly by reducing the secular trend further, making the orbit even more consistent over time. The argument of periapse of the orbit rotates very rapidly, under the influence of the gravitational perturbations. The exciting aspect of this orbit is that the argument of periapse rotates at nearly the same rate as Enceladus rotates about Saturn, making this a Saturn-synchronous orbit. Each time the spacecraft traverses the South Pole, it does so in a very similar direction.

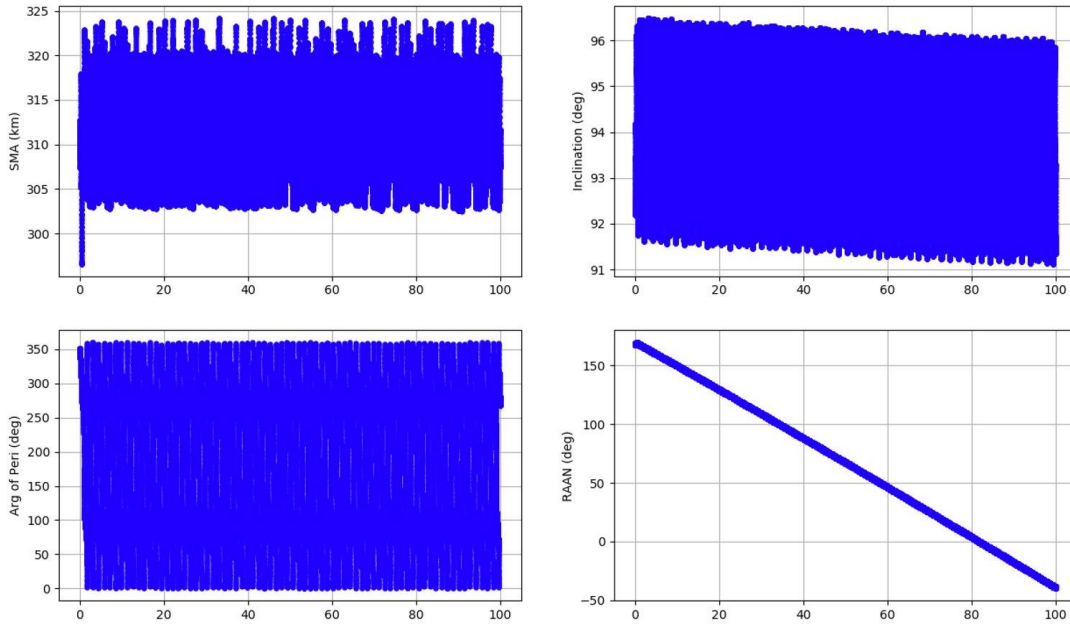


Figure 13 – Several orbital parameters (in an Enceladus-centered J2000 frame) during the primary science mission.

The groundtracks of each science collection passage are shown in Figure 14. This figure illustrates that the geometry of each groundtrack is very similar. Effort has been made to rotate these groundtrack geometries with no success to date. As of this reference, the orbit geometry is very carefully balanced between the groundtrack geometry shown and the resonance of the orbiter and Enceladus about Saturn.

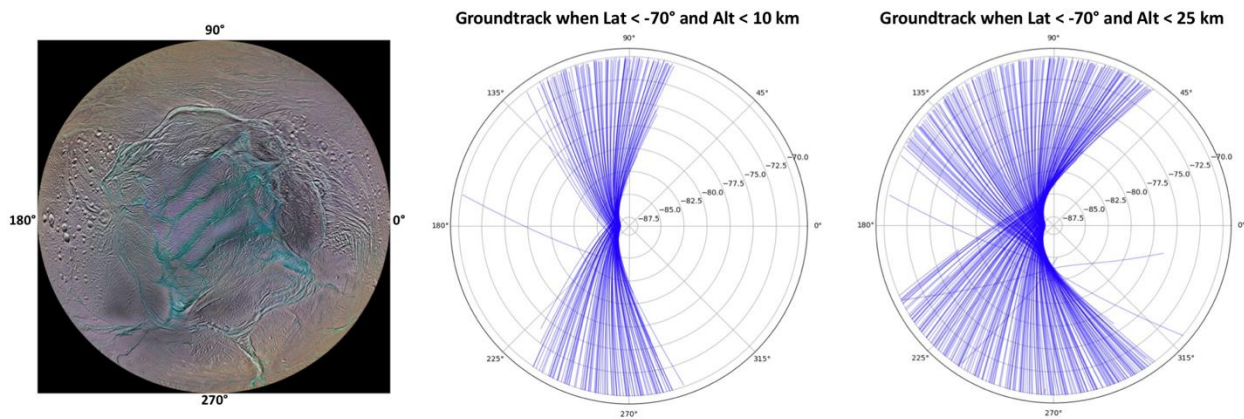


Figure 14 – The groundtracks of each science collection passage, showing each within 10 km (middle) and 25 km (right) for reference.

The science collection occurs when over the Tiger Stripes, so naturally it is desirable for the periapses of the science orbit to pass over the South Pole as often, and as low, as possible. Figure 15 illustrates the locations of the periapses in the IAU Enceladus Fixed coordinate frame. The periapses located below -70 deg in latitude are colored in magenta for all subplots. The first useful observation is that this synchronized elliptical orbit has many such periapse passages. The second observation is that there are a *lot* of periapses located elsewhere: gravitational perturbations cause the argument of periapse (AOP) to rotate rapidly. This further explains the benefit of having a

synchronized AOP precession rate: the 10th periapse always passes over the Tiger Stripes. The longitude bands are further explained by the synchronicity, illustrated in Figure 14.

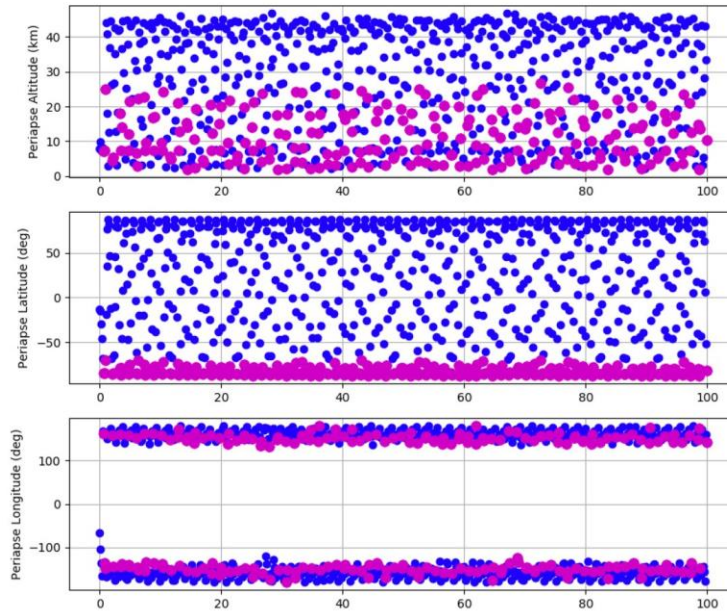


Figure 15 – The locations of the science orbit periapses relative to the Enceladus Fixed coordinate frame.

The periapse passages are not the only points of value: if the periapse occurs prior to a South Pole passage or just afterward, and is low enough, the spacecraft will still pass through useful space. Figure 16 illustrates the altitude of the orbiter over time, with magenta arcs indicating when the spacecraft has a latitude below -70 degrees. One can see immediately how much oscillation there is in the eccentricity of the orbit: the periapse and apoapse altitudes oscillate substantially. The stationkeeping strategy has been formulated to permit the majority of this oscillation without fighting it, but to adjust the time profile carefully to maintain the synchronicity. One can also see that the magenta arcs oscillate from periapse to apoapse and back, which illustrates the synchronicity in the AOP rate. Every 10th orbit has the magenta arc near periapse, and others nearby have low-altitude magenta arcs.

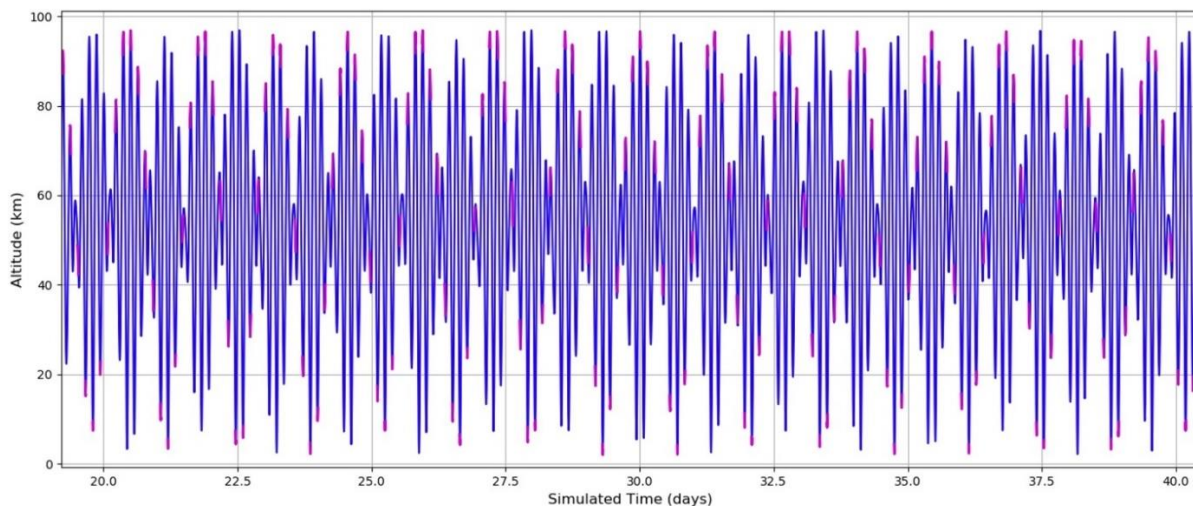


Figure 16 – A plot of the altitude of the science orbit over time; magenta arcs occur when the latitude is below -70 deg.

Figure 17 illustrates the altitude range each time the spacecraft passes below -70 deg in latitude. This provides a distribution of science collection altitudes available over time. This orbit maximizes the time spent below 30 km, but higher altitudes may provide additional scientific samples.

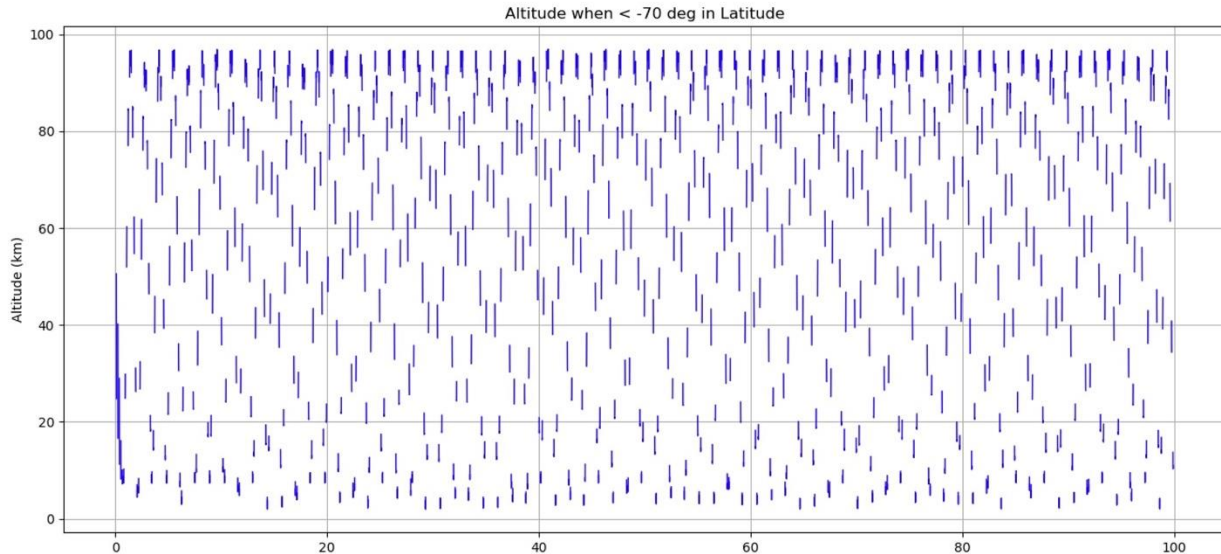


Figure 17 – The altitude range each time the spacecraft passes below -70 deg in latitude.

The ΔV required using the stationkeeping strategy in the reference mission is illustrated in Figure 18. The ΔV at the beginning of the timeline sets up the orbit, which is an opportunity for improvement with future work using a better connection with the orbit insertion sequence. The ΔV usage is very slim for the first 1-1.5 months, and then rises some. It may also be possible to keep the slope lower by adding complexity to the stationkeeping strategy. The slope begins requiring 0.7 m/s per day and then rises to 1.1 m/s per day for an average stationkeeping cost of 0.94 m/s per day. Even without any additional improvement, this time profile demonstrates that a substantial amount of science collection is expected with a relatively low fuel load during these months.

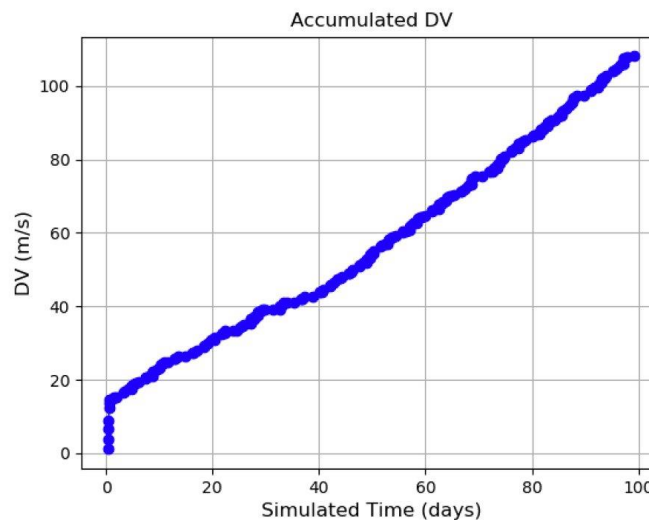


Figure 18 – The accumulated stationkeeping ΔV as a function of time in the reference mission.

Sample Collection Rate

It is desirable to measure the quantity and quality of samples collected in the science orbit. This is done using two relationships, relating the volume of samples collected and the approximate particle size, both as functions of altitude.

As observed in the stationkeeping analyses above, the spacecraft passes over the Tiger Stripes and through their plumes in a variety of geometries. The spacecraft periapse might be located near the Tiger Stripes, but it may also be set before or after the passage through the plumes. For the purpose of this study, the spacecraft passages are modeled as transections through the plumes, with an altitude equal to the altitude the spacecraft passes at its lowest latitude. That is, if the spacecraft groundtrack passed from the North, over near the South Pole at a latitude of -87 deg, and then climbed back upwards again, then the transect altitude is the altitude the observatory had at its lowest latitude, say, -87 deg.

At a 50-kilometer altitude, a 1 m² collector should expect to collect 1.6 μL (microliters) of material per transect⁵. With the expected microbial density based on energetic limitations established from subglacial lake studies, we would need at least 5 imaging sessions to have > 90% probability of detecting a microorganism, if present. The more imaging sessions, the higher we push this probability. And then, with enough sessions, we can start to characterize motility behavior. So, the more the merrier. We will need approximately 31 transects to accumulate enough material in our collection chamber to initiate a microscope imaging session.

The plume density encountered during a transect scales with 1/altitude². However, the expected collected volume scales with 1/altitude, not 1/altitude². This is because the plumes are roughly conical. The length of the transect varies linearly with altitude. So for instance, if at 50 km we can expect 1.6 μL per transect, then at 5 km we can expect 16 μL per transect.

The above is purely a volumetric collection perspective. But there's one more detail that is a bit harder to quantify: particle size. The larger the particles, the lower their apogee. Only small particles are launched at escape velocities. We are expected to encounter 1 micron and smaller particles at 50 km. These particles may be too small to contain any microorganisms, because on the Earth, bacteria and archaea are rarely much smaller than 1 micron, even in energetically limited environments. Calculating particle size vs altitude is very tricky. Some papers have attempted it, but they don't agree very well with each other.

To implement these studies, we used linear relationships that scale as a function of altitude. The volume relationship begins with 10 μL of sample when the transect altitude is 5 km and 1.6 μL of material per transect when the transect is at 50 km. The quality of the sample varies from 1.0 at an altitude of 1 km, when many small organisms could be present in the particles, to 0.0 at an altitude of 50 km (and everything thereafter). This qualitative measure is known as the *goodness* of the sample and generally is a weight of the sample collected during that pass.

⁵ Porco CC, Dones L, Mitchell C. Could It Be Snowing Microbes on Enceladus? Assessing Conditions in Its Plume and Implications for Future Missions. *Astrobiology*. 2017;17(9):876-901. doi:10.1089/ast.2017.1665 <https://www.ncbi.nlm.nih.gov/pmc/articles/PMC5610428/>

Figure 19 illustrates the results of this analysis. First, in the top-left are the transect altitudes of the pass, i.e, the altitude of the Southern-most point in the pass. In the upper-middle are the latitude values that were used in the transect math. The upper-right figure illustrates how many micro-liters are accumulated per pass. The lower-left subfigure accumulates the sample volume per pass into the total volume accumulated to date. Then, the lower-center subplot measures the qualitative goodness of the pass to represent the particle sizes in the sample. Finally, the lower-right subplot illustrates the weighted accumulation of sampled material. One can see that we accumulate approximately 2.5 mL of sample, weighted by the “goodness” factor, over the course of 100 days at Enceladus.

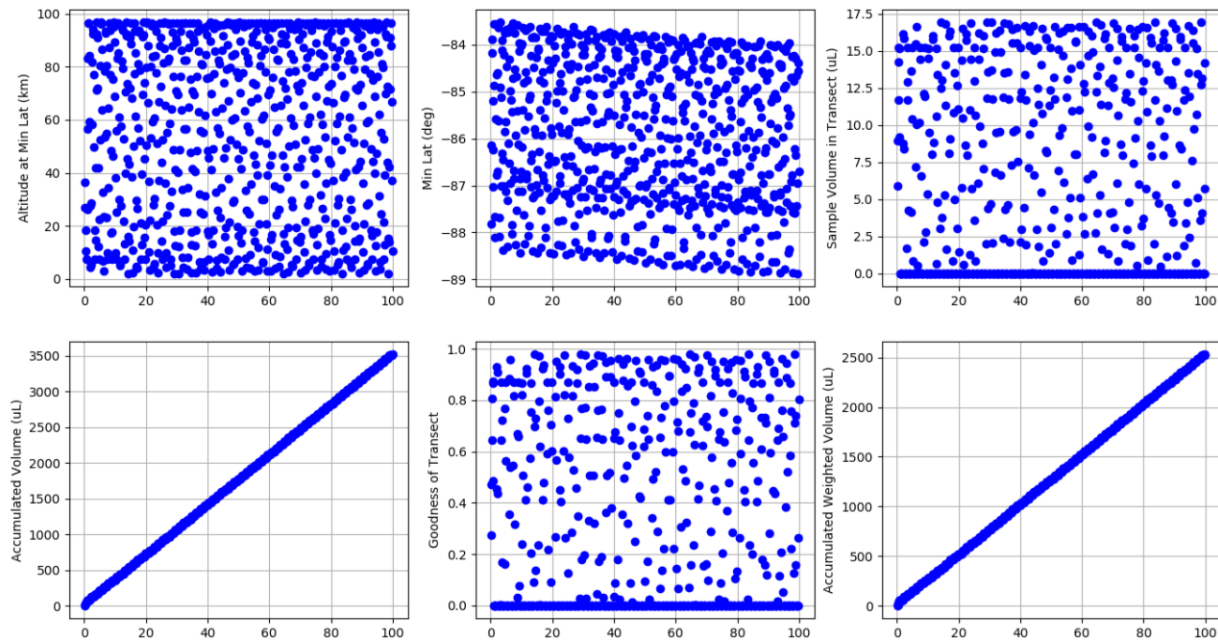


Figure 19. The sample collection results.

Transition to Post-Science Downlink Orbit

Due to the relatively high stationkeeping costs during the science phase of the Enceloscope mission, the baseline mission design assumes the spacecraft will stay in the science orbit for 6-months, then transition to a more stable orbit (that doesn’t require stationkeeping) to downlink the majority of the collected science data. Since Enceladus orbits are highly dynamic and sensitive, and the spacecraft spends a significant portion of its time with Enceladus blocking its view of the Earth, the best option for a post-science orbit is to leave Enceladus orbit and transition to a Saturn-centered orbit. The analysis in this section shows a preliminary design for this transition to get a rough idea of the required ΔV .

Enceloscope can escape the science orbit described above for a minimum of ~ 40 m/s. If this escape maneuver is carefully designed and executed, a trajectory can be found that doesn’t impact Enceladus for at least 10 years. One example of such a trajectory is shown in Figure 20.

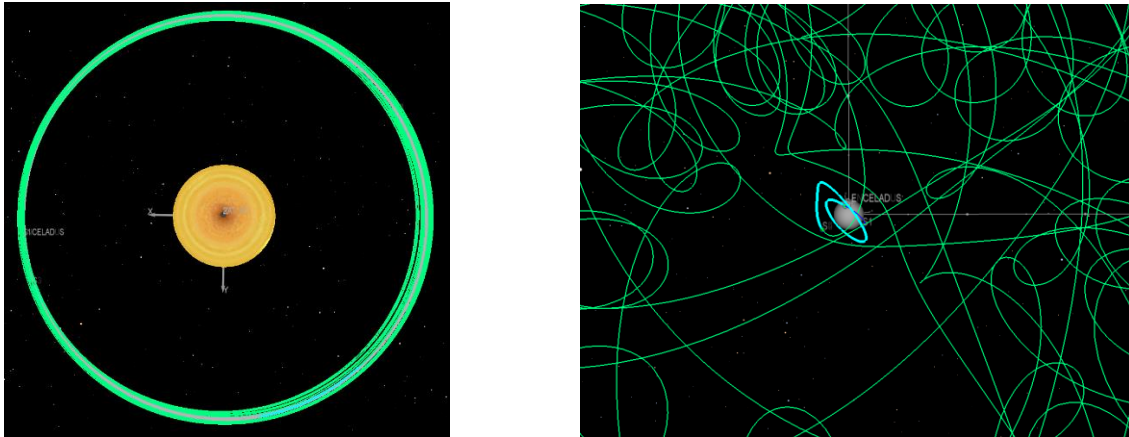


Figure 20 – 10-year propagated trajectory of Enceladuscope after a 42 m/s Enceladuscope-escape maneuver in a Saturn-centered J2000 inertial frame [left] and Enceladus-centered J2000 inertial frame [right].

Although 40 m/s is the minimum ΔV required for leaving Enceladus orbit and entering a Saturn-centered orbit, the resulting trajectory is very sensitive to small perturbations and maneuver execution errors and has several close encounters with Enceladus during the 10-year propagation. If such a trajectory were flown, the spacecraft and/or operators on the ground would need to periodically generate trajectory predictions to ensure those close encounters don't become impacts, and design small maneuvers to avoid them if so. It's estimated that this strategy would require at least another 10 m/s for these small impact-avoidance maneuvers, but that value would be dependent on how far in the future an impact could be predicted and corrected.

A safer, but more ΔV intensive solution is to perform two orbit raising burns after escaping Enceladus' orbit. These maneuvers, each performed as 30 m/s burns in the velocity direction of the spacecraft, raise the Saturn-centered orbit's periapse and apoapse to approximately 241000 km and 246000 km, respectively. While the resulting trajectory, shown in Figure 21, still has close encounters with Enceladus, these encounters are far more distant and less sensitive to small perturbations. This strategy, which requires 100 m/s total for escaping Enceladus and orbit raising, was chosen as the baseline since it significantly reduces the risk of impacting Enceladus and provides a relatively stable orbit for the spacecraft to downlink science data.

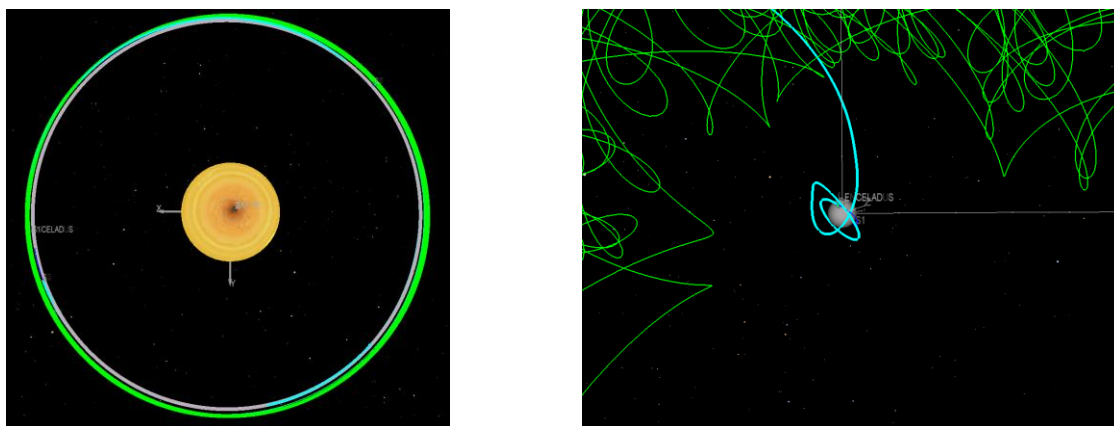


Figure 21 – 10-year propagated trajectory of Enceladuscope after a 42 m/s Enceladuscope-escape maneuver and two 30 m/s periapse and apoapse raising maneuvers in a Saturn-centered J2000 inertial frame [left] and Enceladus-centered J2000 inertial frame [right].

Mission Design Summary

Mission Summary and Deterministic ΔV Budget

The final reference mission design begins in a 200x200 km altitude Earth orbit. After a 4064 m/s injection maneuver on October 5th, 2026, the spacecraft begins its interplanetary journey with flybys of Venus, Venus, and Earth before achieving the energy required to reach the Saturn system. Once arriving at Saturn, on November 12th, 2035, the spacecraft performs a 929 m/s SOI followed by a 524 m/s PRM to target the first Titan flyby and begin the Saturnian moon tour just over 10 years after launch. The moon tour consists of several flybys and maneuvers at Titan, Rhea, Dione Tethys, and finally Enceladus, which aim to reduce the spacecrafts energy relative to Enceladus prior to inserting into the science orbit. In total, 58 flybys are performed along with 20 V_{∞} -leveraging maneuvers during the moon tour, along with 5 maneuvers to transition from one moon to the next. The moon tour takes approximately 3.6 years, and results in a 210 m/s Enceladus orbit insertion on June 17th, 2040. The spacecraft then adjusts its orbit to arrive in the synchronous elliptical orbit and begins collecting science. It collects science several times per day and executes frequent, but small stationkeeping maneuvers. The stationkeeping is simple but must be conducted autonomously. After the science collection phase, the spacecraft will transition to a more stable orbit that doesn't require stationkeeping to downlink the remaining science data. This transition requires a 40 m/s maneuver to leave Enceladus orbit, followed by two 30 m/s burns to raise periapse and apoapse to avoid re-encountering the moon. A summary of the deterministic ΔV , events and time-of-flights for each phase of the mission is provided in Table 24.

Table 24 – Deterministic ΔV and TOF budget.

Mission Phase	Mission Sub-Phase	ΔV [m/s]	Epoch	Duration [days]	Phase Duration [years]
Interplanetary Transfer	Earth Departure	4064.5	05-Oct-2026	3325	10.13
	Interplanetary DSMs	356.5			
	Saturn Orbit Insertion	928.6	12-Nov-2035	75	
	Periapse Raising Maneuver	524.1	26-Jan-2036	297	
Moon Tour	Titan Tour	46.1	18-Nov-2036	115	3.58
	Rhea Tour	449.0	13-Mar-2037	613	
	Dione Tour	364.4	16-Nov-2038	184	
	Tethys Tour	364.6	19-May-2039	202	
	Enceladus Tour	104.4	07-Dec-2039	194	
	Enceladus Orbit Insertion	211.0	17-Jun-2040		
Science	Stationkeeping	180.0		180	0.5
	Transition to Post-Science Orbit	100.0	17-Dec-2040		
Total		7693.2		5185	14.21

Statistical ΔV and Mass Budgets

In addition to the summarized deterministic ΔV budget above, a statistical ΔV budget is provided in Table 25. This budget includes margin for launch/injection, maneuver execution, and navigation

errors as estimated by the interplanetary and (TBC) moon tour statistical ΔV analyses. A placeholder value of 665 m/s has been set for the moon tour, representing roughly 50% of the total ΔV for that phase of the mission. This estimate is based on analysis that concluded that the interplanetary phase required 48% additional ΔV .

Table 25 – Statistical ΔV Budget

Mission Phase	Mission Sub-Phase	ΔV [m/s]
Interplanetary Transfer	Earth Departure	4064.5
	Interplanetary DSMs	356.5
	Saturn Orbit Insertion	928.6
	Periapse Raising Maneuver	524.1
	Phase ΔV Margin	297.3
Moon Tour	Titan Tour	46.1
	Rhea Tour	449.0
	Dione Tour	364.4
	Tethys Tour	364.6
	Enceladus Tour	104.4
	Enceladus Orbit Insertion	211.0
	Phase ΔV Margin	850
Science	Stationkeeping	180.0
	Transition to Post-Science Orbit	100.0
	Phase ΔV Margin	28.0
Total		8868.5

The largest component of the ΔV budget is the interplanetary injection (or Earth departure) maneuver, which at 4064.5 m/s makes up 46% of the total statistical budget. Given this, it is important to understand how this ΔV may change if Encelascope is launched to a higher orbit than the baseline 200x200 km altitude low-Earth orbit. Figure 22 illustrates this trade, showing how the injection ΔV varies with apogee altitudes from 200 to 50000 km.

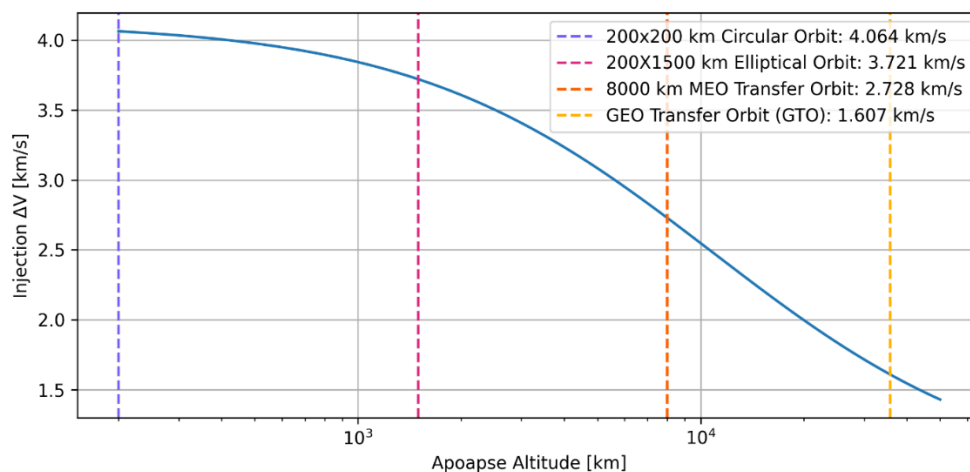


Figure 22 – Interplanetary injection ΔV as a function of the initial orbit's apoapse altitude (assuming a 200 km altitude periapse).

From Figure , three example initial orbits were selected to build mass budgets. These initial orbits include the baseline 200x200 km altitude low-Earth orbit, an elliptical 200x1500 km altitude orbit, and a Geostationary Transfer Orbit (GTO) with an apogee altitude of 35786 km. In addition, a mass budget is built for a spacecraft that gets a direct launch to the interplanetary injection, without the need for the first stage. The assumed spacecraft staging and propulsion parameters are listed in Table 26 and mass budgets are shown in Table 27 through Table 30.

Table 26 - Spacecraft mass and Isp assumptions.

Stage	Components	Isp [sec]	Stage Dry Mass
1	Propellant Tank and Engine	335	9%
2	Propellant Tank and Engine	335	11%
3	Propellant Tank and Engine	335	13%
4	Spacecraft and Engine	280	45.6 kg

Table 27 - Mass budget assuming launch into a 200x200 km altitude Earth orbit.

200x200 km Altitude			Mass [kg]		
Stage	Mission Phase	ΔV [m/s]	Wet	Propellant	Stage Dry
1	Injection	4064.5	1203.8	854.3	84.0
2	Transfer, SOI and PRM	2106.5	265.5	125.6	15.5
3	Moon Tour	2178.5	124.3	60.3	9.0
4	EOI, Science, Post-Science	519.0	55.1	9.5	45.6

Table 28 - Mass budget assuming launch into a 200x1500 km altitude Earth orbit.

200x1500 km Altitude			Mass [kg]		
Stage	Mission Phase	ΔV [m/s]	Wet	Propellant	Stage Dry
1	Injection	3721.0	1040.9	705.4	70
2	Transfer, SOI and PRM	2106.5	265.5	125.6	15.5
3	Moon Tour	2178.5	124.3	60.3	9.0
4	EOI, Science, Post-Science	519.0	55.1	9.5	45.6

Table 29 - Mass budget assuming launch into a Geostationary Transfer Orbit (GTO).

GTO			Mass [kg]		
Stage	Mission Phase	ΔV [m/s]	Wet	Propellant	Stage Dry
1	Injection	1607.0	461.8	178.6	17.7
2	Transfer, SOI and PRM	2106.5	265.5	125.6	15.5
3	Moon Tour	2178.5	124.3	60.3	9.0
4	EOI, Science, Post-Science	519.0	55.1	9.5	45.6

Table 30 - Mass budget assuming launch directly to the interplanetary injection.

C3 = 19.16 km²/s²			Mass [kg]		
Stage	Mission Phase	ΔV [m/s]	Wet	Propellant	Stage Dry
1	Injection	0.0	0.0	0.0	0.0
2	Transfer and Moon Tour	2106.5	265.5	125.6	15.5
3	Moon Tour	2178.5	124.3	60.3	9.0
4	EOI, Science, Post-Science	519.0	55.1	9.5	45.6

Launch Options

The mass budgets in the tables above can now be compared with the capabilities of candidate launch vehicles for the mission. ASTROBi identified the ABL RS-1 launch vehicle as an ideal choice given the promised low cost and high performance. With the 4-stage spacecraft design, Enceloscope can be launched into a 200x200 km orbit by the ABL RS-1 with 146.2 kg of excess capacity. Alternate options identified include the Indian PSLV G, which has the capacity to launch 1150 kg to a GTO (leaving 688.2 kg of margin for an Enceloscope mass of 461.8 kg) or the European Space Agency’s VEGA, which has the capacity to launch 1963 kg to a 200x1500 km altitude orbit (leaving 992.1 kg of margin for an Enceloscope mass of 1040.9 kg). Although both these launch vehicles are more expensive than the ABL RS-1, they have a proven record and offer significant margin. The extra capacity available on either vehicle could also be sold to a secondary payload, such as one going to Venus, making this option more economical.

Table 31 - Example launch vehicles and mass margin.

Launch Vehicle	Orbit [km]	Payload Capacity [kg]	Enceloscope Mass [kg]	Margin [kg]	Est. Cost
ABL RS-1	200x200	1350	1203.8	146.2	\$10+ mil
ABL RS-1	GTO	320	461.8	-141.8	\$10+ mil
PSLV G	GTO	1150	461.8	688.2	\$21-31 mil
VEGA	200x1500	1963	1040.9	992.1	\$37 mil

Conclusion

The results and analyses presented here culminate in an end-to-end mission design for a low-cost science mission to Enceladus launching in October of 2026. The mission design was developed with a focus on minimizing the required spacecraft ΔV while beginning science in or before 2040. The result is a complex, long time-of-flight, but feasible trajectory design consisting of a Venus-Venus-Earth multi-gravity assist interplanetary transfer, a Saturnian moon tour that leverages flybys of Titan, Rhea, Dione, Tethys and Enceladus, and a science orbit and stationkeeping strategy that maximize plume material collection with minimal propellant use. The interplanetary and moon tour trajectories were first developed using low-fidelity methods before transitioning to higher-fidelity trajectory models.

The interplanetary transfer was designed by performing a global optimization search of multi-gravity assist transfers between Earth and Saturn, utilizing several combinations of Earth and Venus flybys to minimize the spacecraft ΔV . This search was implemented with a simplified trajectory model using only 2-body dynamics. A Venus-Venus-Earth transfer, launching in October 2026 and arriving at Saturn 9 years later in November 2035, was selected as the reference mission design due to its minimal deep space maneuver ΔV and relatively short time-of-flight. The low-fidelity solution was verified and re-optimized in a high-fidelity trajectory model, with the resulting trajectory closely matching the low-fidelity solution. After a Saturn Orbit Insertion maneuver, a Periapse Raising Maneuver was designed to target a flyby of Titan and kick-off the extensive moon tour. The deterministic ΔV budget for the interplanetary transfer, including the injection ΔV from a low-Earth orbit, SOI and PRM was found to be 5873.7 m/s, with an additional 297.3 m/s of ΔV allocated to account for statistical launch/injection, maneuver, and navigation errors.

The moon tour was designed using the low-fidelity Tisserand and V_∞ leveraging methods which make several simplifying assumptions but enable the design of a complex and near-optimal series of flybys that reduce the spacecrafts energy relative to Enceladus for a minimal amount of ΔV . The tour at each Saturnian moon (Titan, Rhea, Dione, Tethys and Enceladus) was designed and optimized independently, first in the low-fidelity model before conversion to a high-fidelity trajectory. In general, the low-fidelity solution provided a good initial guess for the high-fidelity trajectory, with the flybys and maneuvers matching closely. A significant portion of the ΔV required for the moon tour came not from the individual tours themselves, but from the transitions between each moon. This ΔV could likely be reduced by optimizing the moon tours together, but the individual optimization of moon tours proved to already be a complex and computationally challenging task. In total, the final moon tour includes 58 flybys and 24 deterministic maneuvers prior to insertion into orbit around Enceladus. The deterministic ΔV budget for this phase of the mission is 1328.5 m/s, with an additional 850 m/s allocated for the statistical ΔV budget and 211 m/s for insertion into Enceladus orbit. The moon tour's series of flybys is the most complex and highest risk phase of the mission. Each flyby is highly dependent on the flybys before it, so any missed or poorly executed maneuver or flyby will likely necessitate a non-trivial redesign of the remaining moon tour. Given the limited timeline between some of the flybys and deterministic maneuvers, a spacecraft anomaly that delays any one of these events by mere days could lead to a complete redesign of the remaining mission and may delay Enceladus arrival by several months. To mitigate this risk, the spacecraft and navigation concept of operations should be designed and tested to be robust to such anomalies, and ground operators should be prepared to quickly re-optimize the moon tour from any point in the mission.

The Enceladus science orbit was selected from a trade of several options that considered the predicted plume material collected (based on the spacecraft's altitude and time spent at low latitudes) and stationkeeping costs. An elliptical orbit was discovered that has a 10:1 resonance with Enceladus' orbit around Saturn, placing every 10th periapse over the Tiger Stripes. A stationkeeping strategy was developed that can maintain this orbit for approximately 1 m/s of ΔV per day. Second only to the moon tour, this phase of the mission also introduces a fair amount of risk. The science collection requirements necessitate a low-altitude trajectory, which can quickly evolve to be an impact trajectory in the highly perturbed environment around Enceladus (primarily due to Saturn's gravitational influence) without stationkeeping. During this phase of the mission,

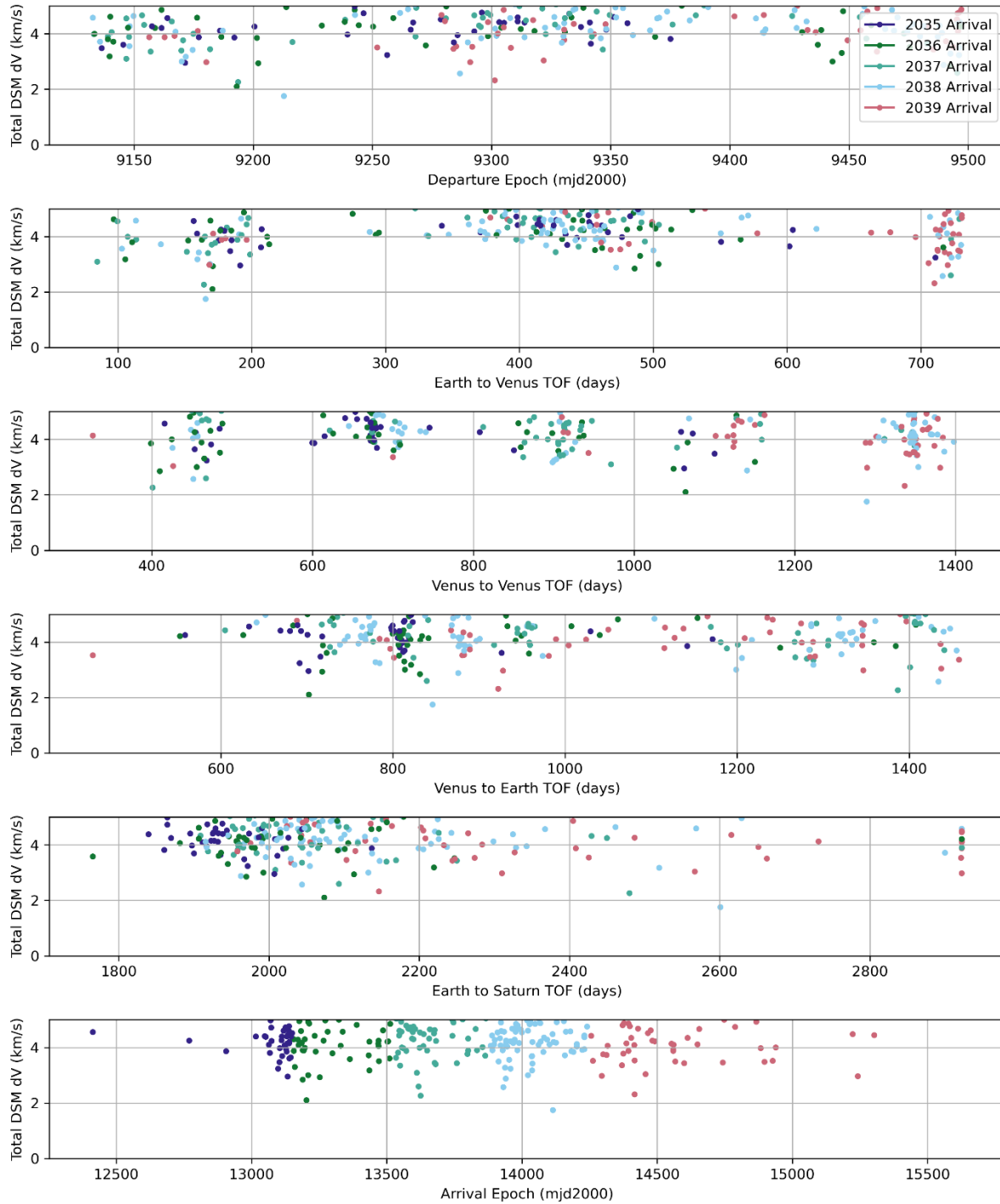
the spacecraft will have to have consistent and good knowledge of its state and must always be prepared to execute a stationkeeping or collision avoidance maneuver.

The final trajectory design, which has a total time-of-flight of just over 14 years, requires 7693.2 m/s of deterministic ΔV and an estimated 1175.3 m/s for statistical margin. This results in a total ΔV budget of 8868.5 m/s. Given this final trajectory design and ΔV budget, mass budgets were developed for a 4-stage spacecraft design and several launch options were considered. The most promising low-cost option was found to be a launch on an ABL RS-1 vehicle to a low-altitude, 200x200 km, parking orbit. With this option, a 4-stage spacecraft with a wet mass of just over 1200 kg and an Isp of 335 sec would carry the propellant necessary, with margin for trajectory correction maneuvers, for the end-to-end Enceladus mission design presented here.

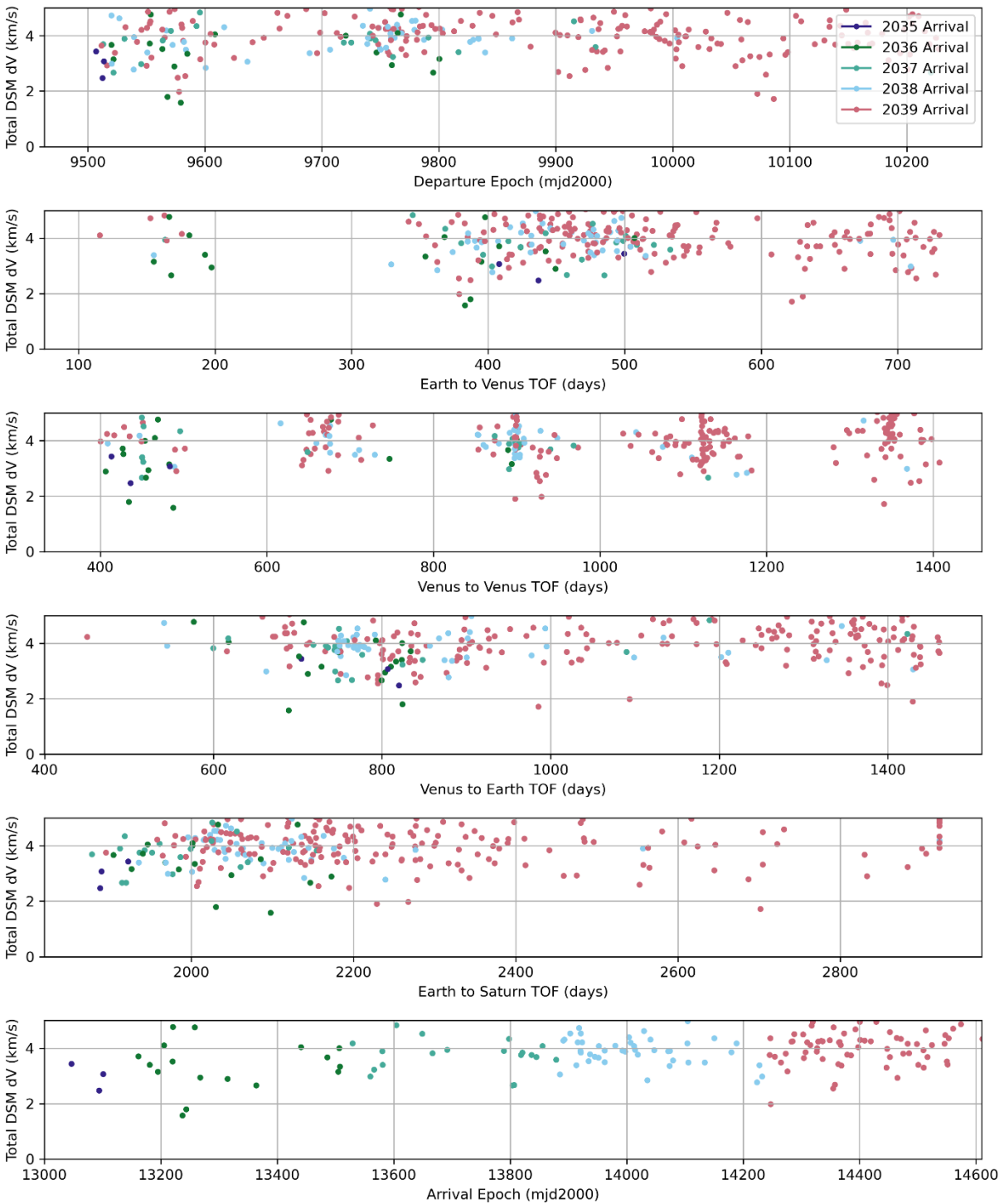
Appendix

Results from Interplanetary Transfer Global Search with pykep and pygmo

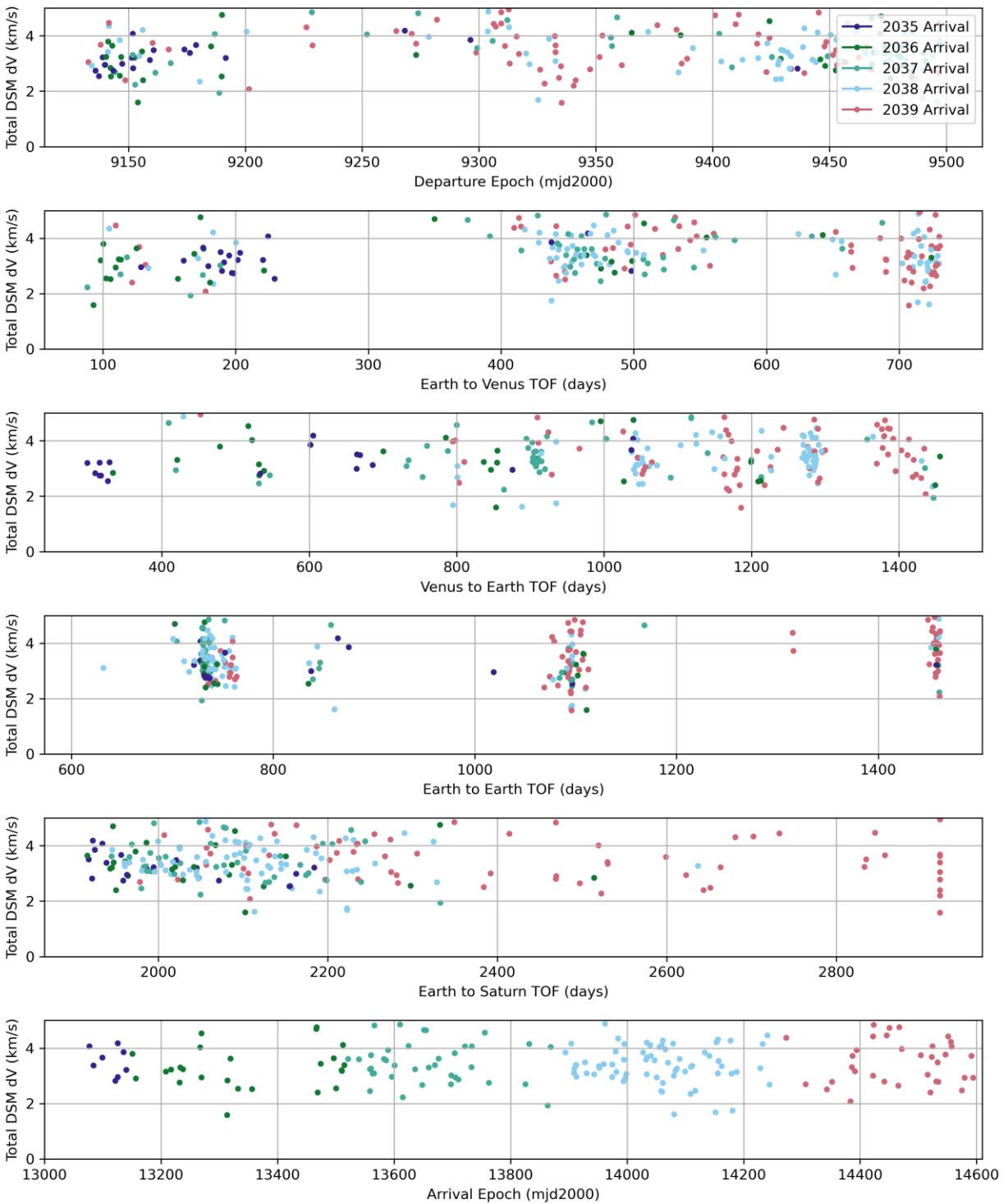
EVVES Transfers Departing in 2025



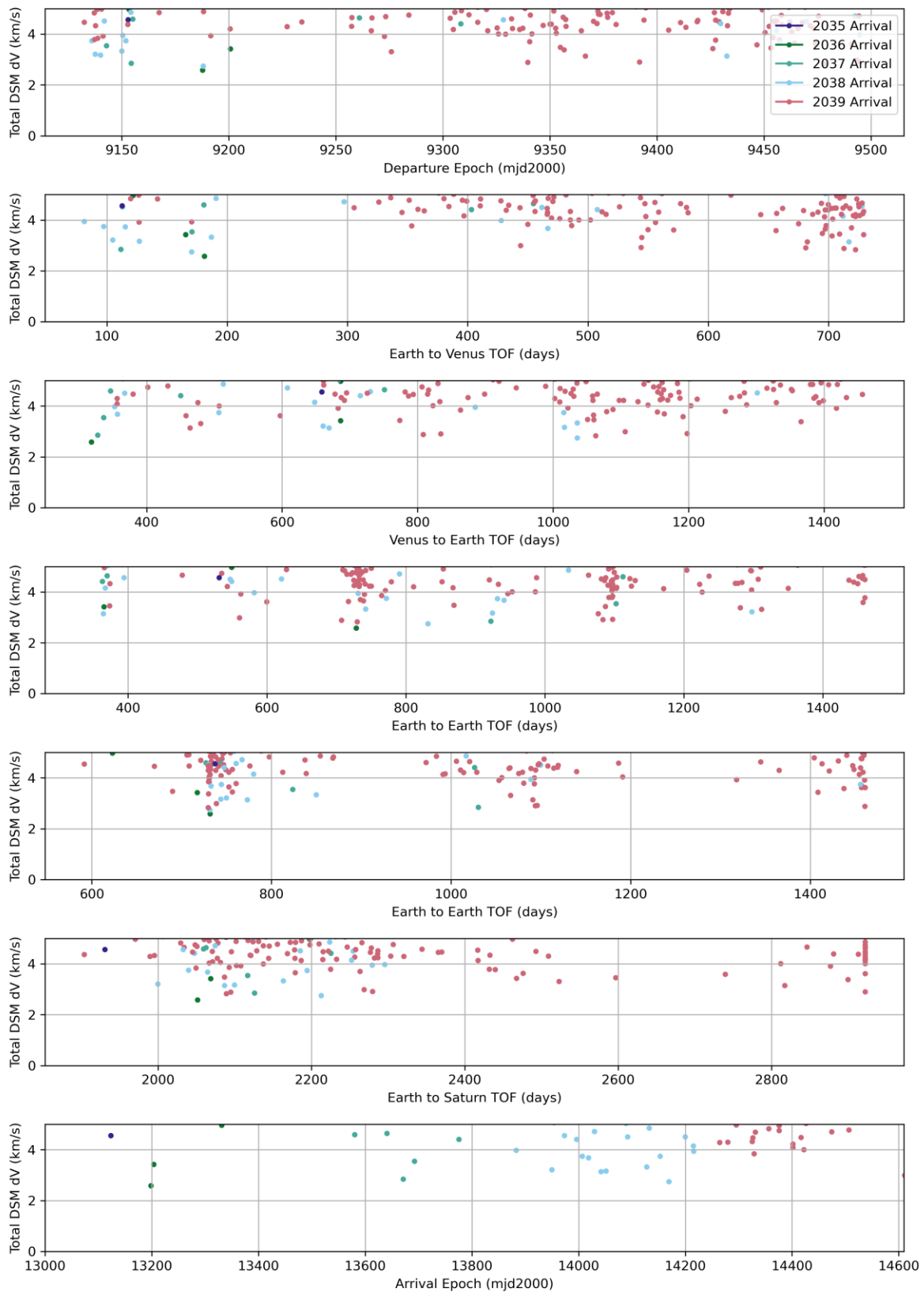
EVVES Transfers Departing in 2026



EVEES Transfers Departing in 2025



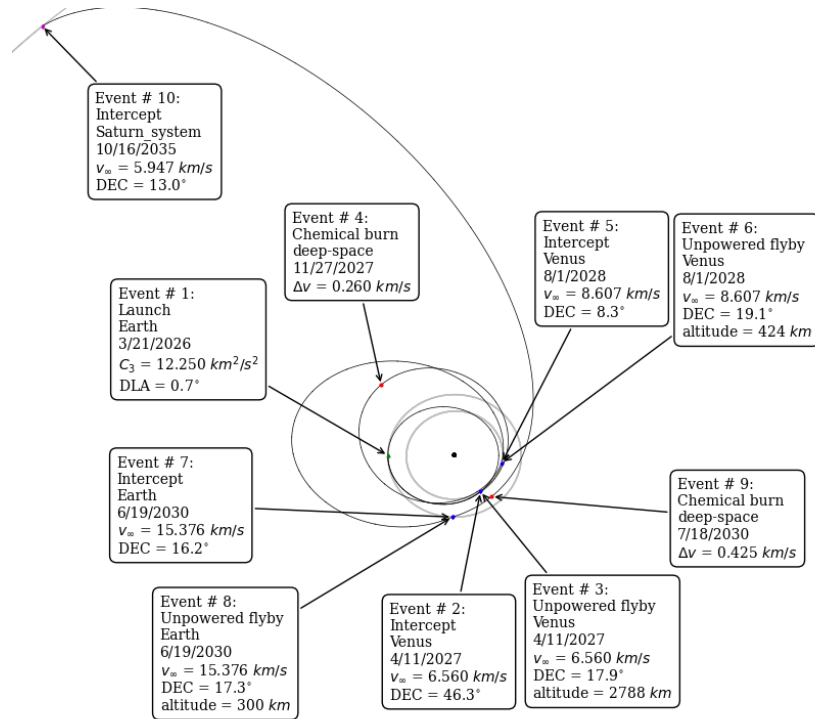
EVVEES Transfers Departing in 2025



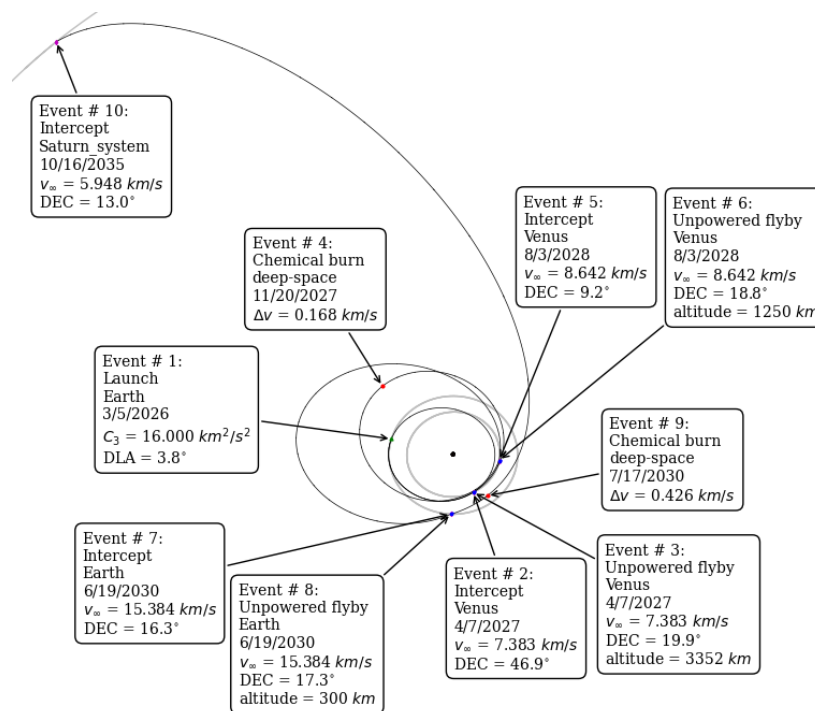
EMTG Interplanetary Transfer Solutions

EVVES Palma ID5 Transfer

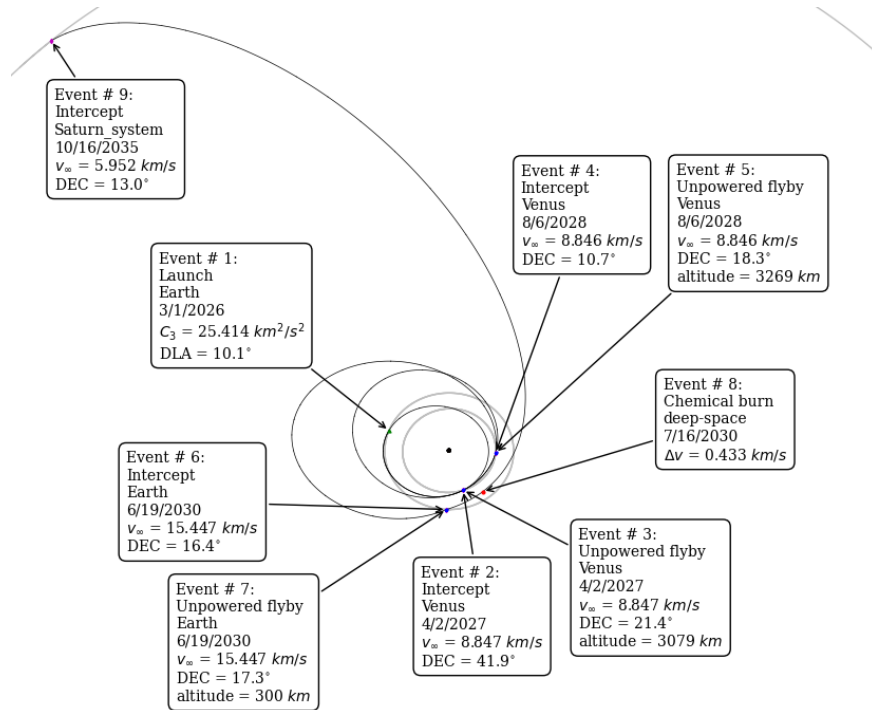
$V_{\infty} = 3.5 \text{ km/s}$



$V_{\infty} = 4.0 \text{ km/s}$

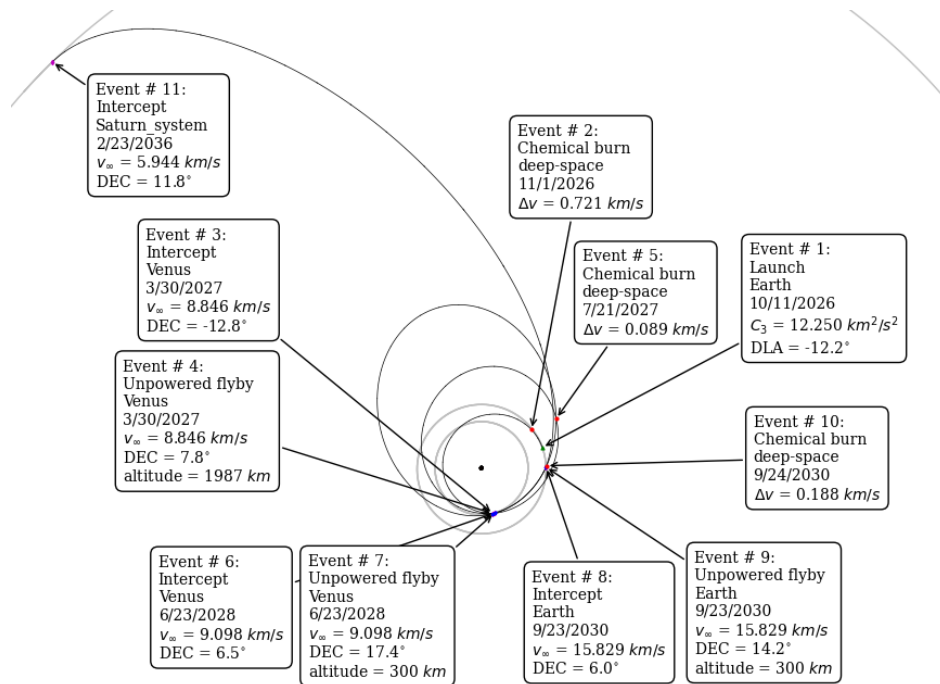


$V_{\infty} = 5.0$ km/s (unconstrained)

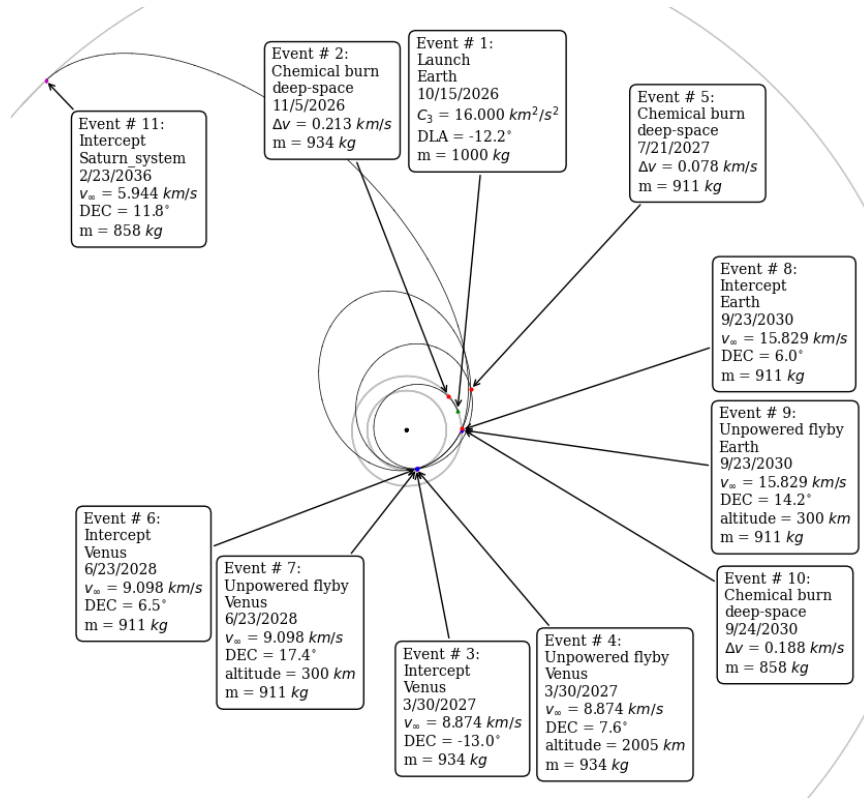


EVVES Palma ID6 Transfer

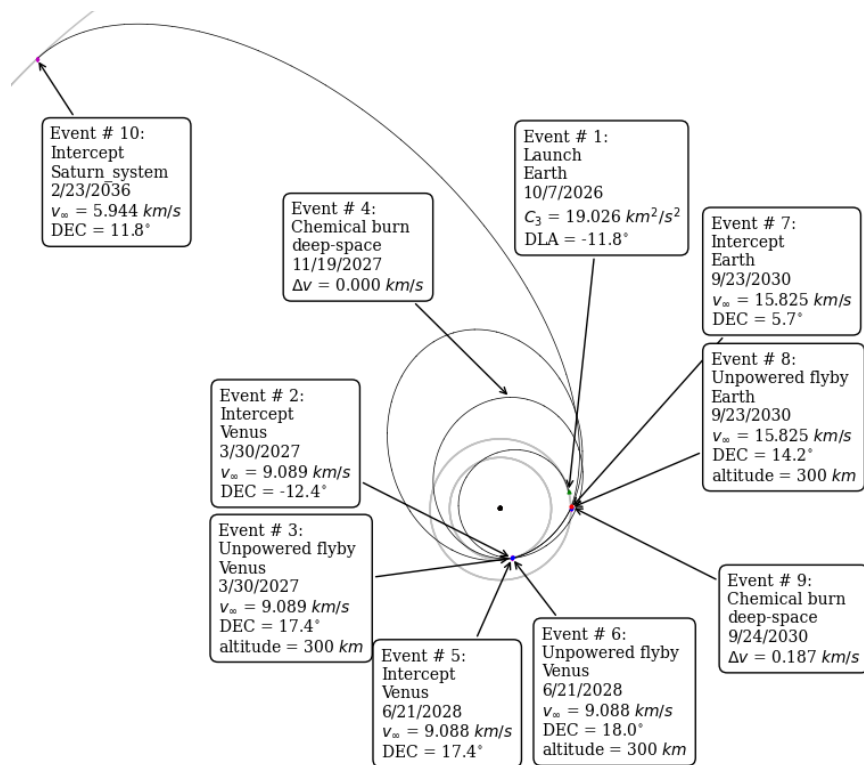
$V_{\infty} = 3.5$ km/s



$V_{\infty} = 4.0 \text{ km/s}$

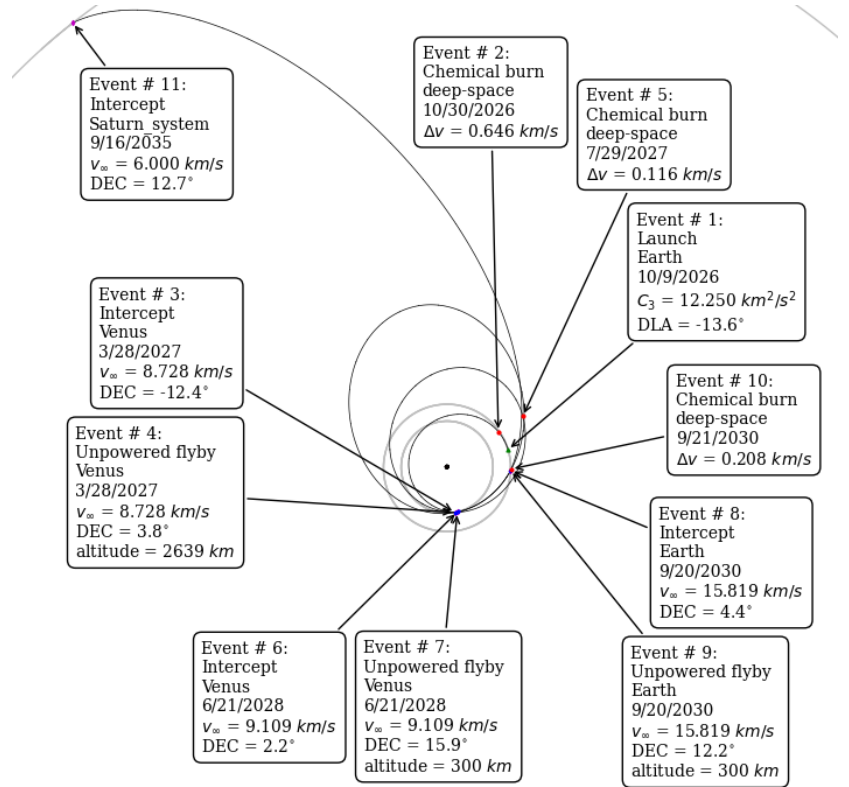


$V_{\infty} = 4.36 \text{ km/s}$ (unconstrained)

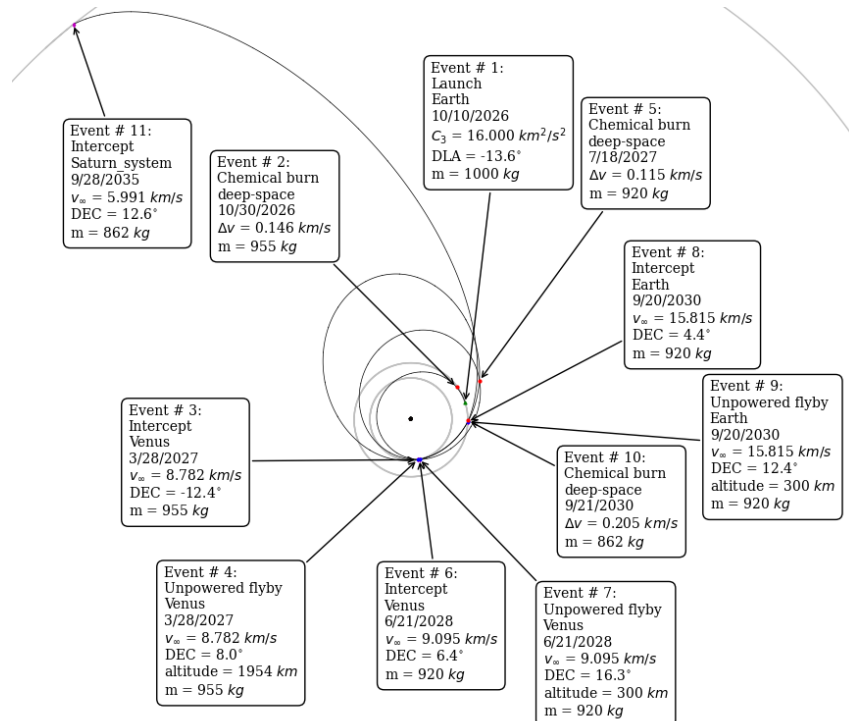


EVVES Palma ID7 Transfer

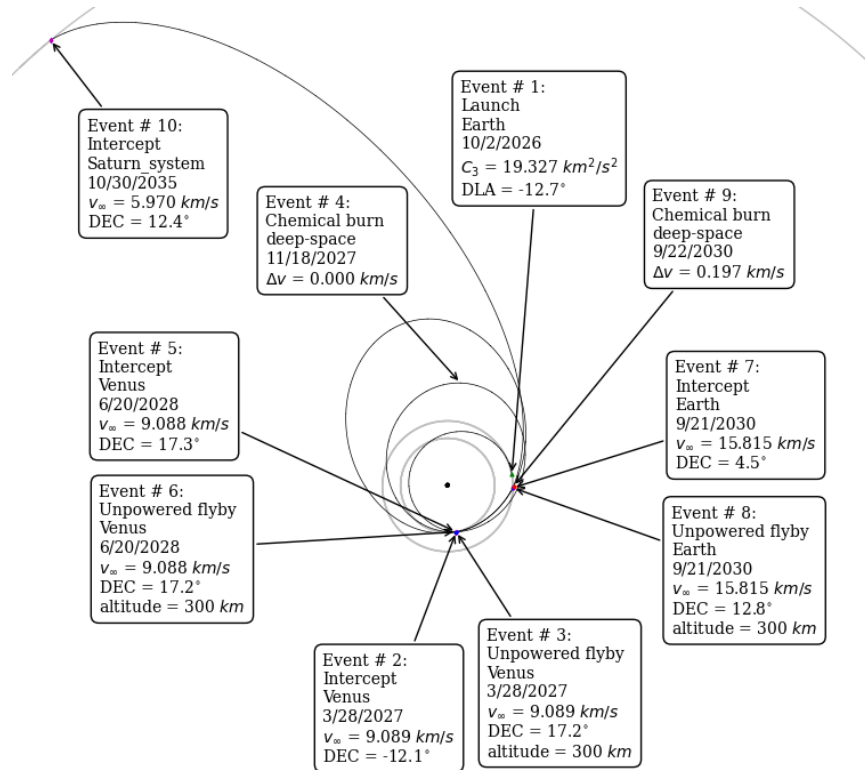
$V_{\infty} = 3.5 \text{ km/s}$



$V_{\infty} = 4.0 \text{ km/s}$

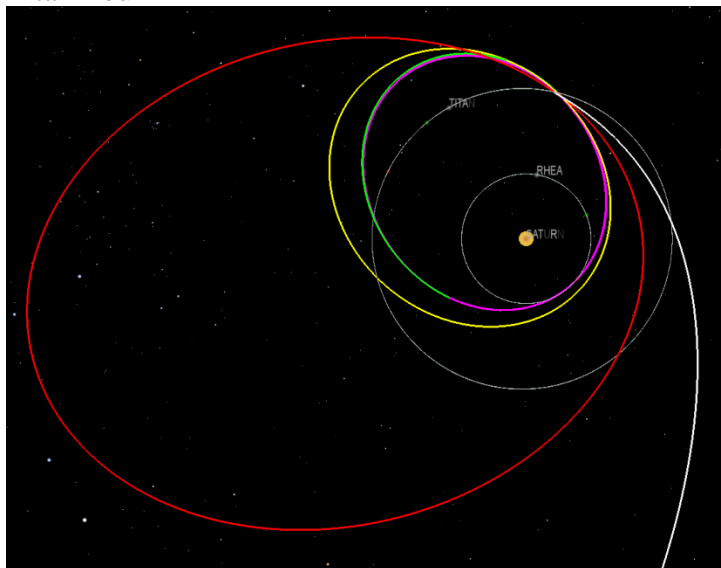


$V_{\infty} = 4.36 \text{ km/s}$ (unconstrained)

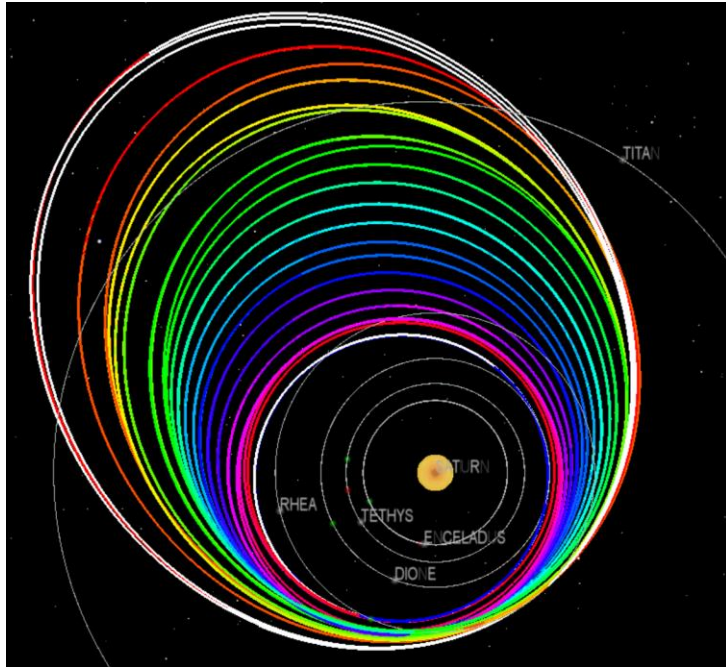


High-Fidelity Moon Tour Trajectories

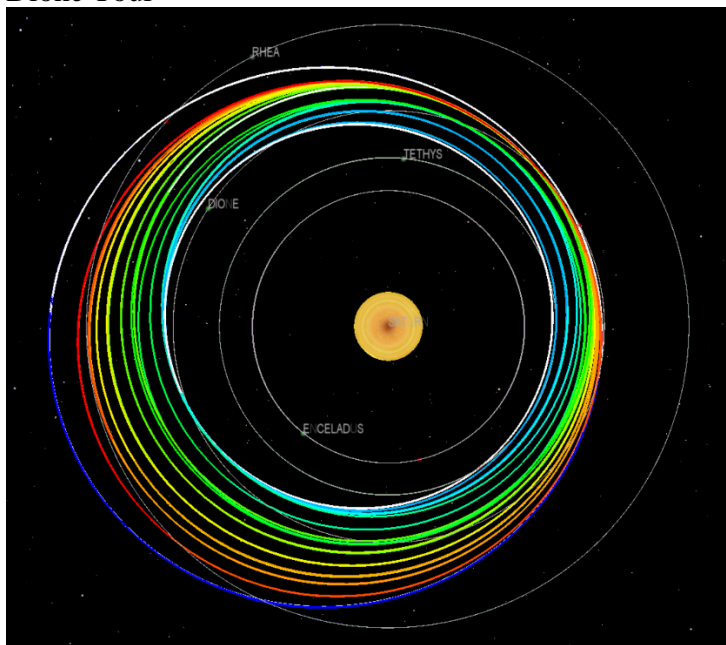
Titan Tour



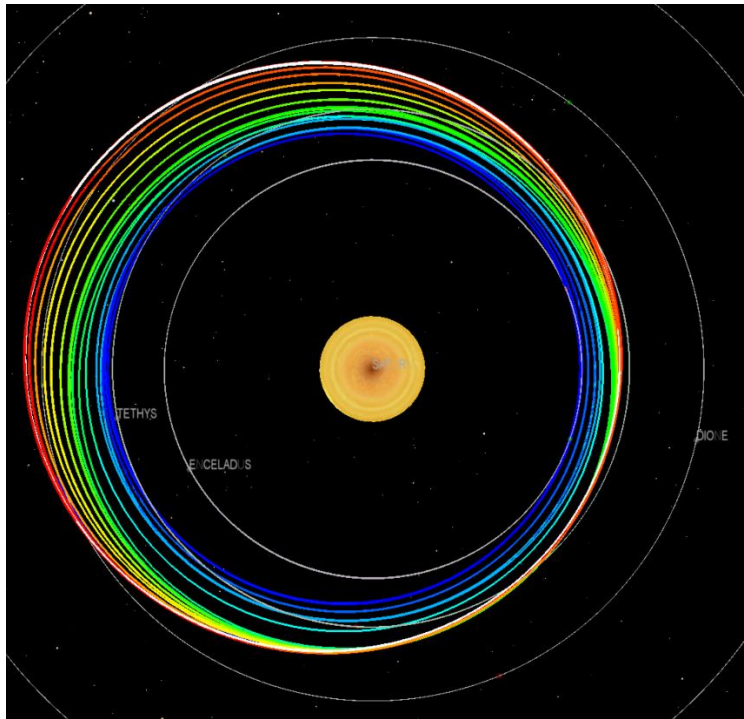
Rhea Tour



Dione Tour



Tethys Tour



Enceladus Tour

